Heat Transfer Study for Estimating Temperature Distribution inside the Sample Environment of a Helium Gas Cryocooler

Submitted by

Faycal Diallo

in partial fulfillment of the requirements for the degree of

Master of Science

in

Mechanical Engineering

Tufts University

May 2016

Certified By …… Dr. Luisa Chiesa, Associate Professor, Department of Mechanical Engineering, Tufts University

Certified By …….Dr. Behrouz Abedian, Associate Professor, Department of Mechanical Engineering, Tufts University

Certified By …….Dr Makoto Takayasu, Research Scientist, Plasma Science and Fusion Center, Massachusetts Institute of Technology

Abstract

The superconductive character of a material is mainly dependent on three factors, one of which is temperature. The exceptional feature about superconductors is that once current is setup in them, it can persist in superconducting loops virtually for several years without decay given the adequate conditions of temperature, current density and magnetic field. In this thesis we discuss the thermal characteristics inside the cryocooler utilized in testing High Temperature Superconducting (HTS) materials. The test sample is cooled to temperatures as low as 4.2 K in a space filled with helium gas. Prior experiments were conducted using liquid nitrogen and therefore only tested to 77 K. The opportunity to use helium gas instead of liquid cryogens such as liquid nitrogen and helium, offers a more flexible and safer environment. The cooling in a cryocooler system is mainly driven by conduction and convection heat transfer through the helium gas, therefore it is generally not as good as a cryogenic liquid in removing heat produced during an experiment. To verify that the system can be properly utilized for the planned experiments, it became necessary to estimate the temperature distribution in the cryostat when a typical thermal load such as the test rig hardware is placed in the sample area of the cryocooler. An analysis using finite element model was sought to provide answers regarding the temperature profile. The results demonstrated that the amount of mass and material properties of the test rig elements can affect the temperature distribution. These finding can help in designing test hardware adequate for a given test requirements.

Acknowledgement

I would like to express my deepest appreciation to my advisor professor Chiesa for her patience and mentorship as I worked through the process of completing my master thesis project. It was a challenge to balance work, school and family but she always understood, when we have to change a meeting time or reschedule because of a conflict.

A very special thank you to Dr. Makato Takayasu who provided valuable feedback during review session that were held, to go over thesis progress. He managed to come after hour and he stayed way past normal business hours to support this work. Also thank you for gracefully accepting to be part of my review committee.

A very special thanks to Prof. Abedian for accepting to be part of my review committee and for all the feedback he has provided me in helping to hash out his paper.

A special thank you to my manager Kevin Mcmanus, who allowed me to flex between work and school hours so I can finish my thesis despite a very demanding scheduling at work.

Georgios Karamanis, has been a great help with teaching me how to use the ANSYS Fluent tool. He would take out time from his busy schedule and sometimes will stay until late at night to help debug my code. Great thanks.

Great thanks to Richard Barrett for his mentorship. He is a great inspiration. He would always ask me when we meet in the hallway at work: “Has it gotten cold enough yet” in reference to the cryocooler. He is a senior design engineer at GE and had seven years of cryogenics experience under his belt prior to joining GE. He has provided valuable insight in term of designing a test rig that supports testing for carrying current capacity and tension testing of a superconductor sample using the cryocooler we have in the lab.

I would like to also thank my laboratory colleague Federica Pierro, for gracefully accepting to share her experimental findings conducted with the cryocooler. It allowed me to make a correlation with some of my simulation results.

I cannot express enough gratitude to my wonderful wife for her patience and resilience. Every time, I will call her to tell her that I would be late that night she would not complain. She has been very supportive throughout the process while taking care of our few months old boy.

At last I would like to thank my family members for their support and especially to my mother who always prayed for the completion of my master degree.

Table of Contents

List of Figures

List of Tables

Chapter I: Introduction

Superconductors are materials that will conduct electricity without resistant when they are below a certain temperature known as critical temperature. This phenomenon was not discovered until Dutch physicist Heike Kamerlingh-Onnes noticed that when the temperature of mercury was lowered to 4.2 K, the resistance of the sample he was studying suddenly dropped to zero.

Onnes also discovered that superconducting material will exhibit such properties under the appropriate condition. The appropriate condition is a function of temperature as mentioned earlier, but also magnetic field and current. The effect of the governing parameters can be plotted in a diagram known as a critical surface as shown in figure 1.

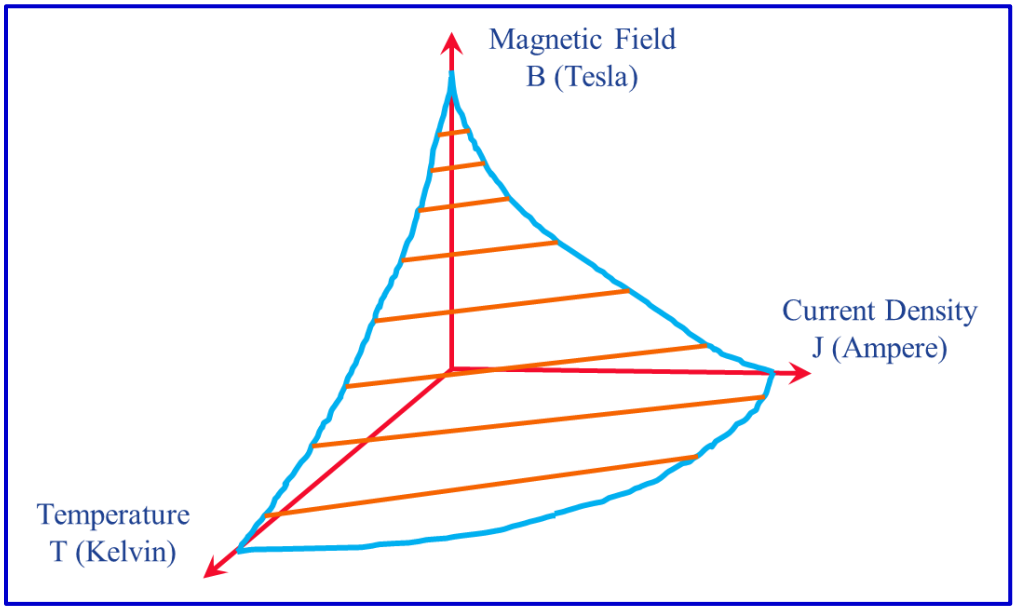

Figure 1. Sketch of the critical surface of a superconductor

The applied magnetic field (B), temperature (T) and the current density (J_0) must remain below the critical surface in order for the material to remain in a superconductive state. In the event that any of the three parameters increase to a level above the critical surface, the material will promptly lose its superconductive property.

Superconducting materials are classified in two groups, Low Temperature superconductor (LTS) and High Temperature Superconductors (HTS). LTS have a critical temperature that is less than 77 K, on the other hand HTS (High Temperatures Superconductor) such as YBCO and BSCCO will exhibit superconducting properties at temperature as high as 138 K. The transition temperature of 77 K represents the boiling point of liquid nitrogen at atmospheric pressure. LTS would therefore require using a fluid which has a lower boiling point that nitrogen in order to reach their critical temperatures. Low Temperature Superconductors are typically cooled in liquid helium where a temperature of 4.2 K can be reached.

Superconductor applications are found in high energy physics and fusion energy research, aeronautics, medical devices, power distribution and storage and in the field of transportation for high speed train.

1.1 Application of Superconductors

1.1.1 High-Field Superconducting Magnets Applications

Superconducting magnets have a clear advantage over ordinary ferromagnetic-core electromagnets, because they can generate magnetic fields that are up to ten times stronger. These types of magnets are smaller and consume much less power, with an empty hollow core which can lend itself to the particle accelerator applications that are ongoing around the world. Without such magnets, the discoveries at the Large Hadron Collider LHC facility would not have been possible. The LCH with its 27 kilometers in circumference made out of a ring of superconducting magnets stands as the world’s largest and most powerful particle collider.

The other application for these high field superconducting magnets is fusion energy. In this application fusion power is generated through fusion nuclear reactions between charged particles in a plasma. High magnetic fields are used to confine the plasma. The magnetic confinement of fusion is seen as the most promising approach because of the quality of the results that can be generated and the abundance of the energy source. The ITER machine under construction in France [1] has been the driving force behind such research in trying to prove the feasibility of fusion energy for power generation. ITER has been mainly the motivation behind the research conducted at the Tufts superconducting laboratory.

1.1.2 Aerospace Applications

Studies have been conducted by researchers to determine the possibility of using high T_c superconducting materials for launching aircraft through magnetic levitation [2]. The approach for launching aircraft will be to attach the aircraft via a quick disconnect device, such as the one used on aircraft carriers, to an electromagnetic shuttle that behaves like a catapult. The electromagnetic catapult system is directly attached to the underbody of the aircraft. The use of superconducting HTS is certainly the most probable near term application of aircraft launch aboard naval carriers. Today, this electromagnetic aircraft launch system is a design feature on the latest USS Gerald T. Ford aircraft carrier [3], even though it has not been confirmed that superconductors are used in the electromagnetic launch system.

1.1.3 Medical Applications

Superconducting material have become an essential element in the field of healthcare through Magnetic Resonance Imaging more commonly known as MRI. MRI is used as a non-invasive way of diagnosing patient for abnormalities inside the human body. MRI was discovered in the mid-1940s but it took until 1977 for the first exam to be conducted on a human being. That first MRI took five hours to produce, in the fast computer days that we live in, it takes much less time. The principle of operation of the MRI relies on the superconducting magnet to provide the background field and RF coils excites the hydrogen atom that are present in the water molecules and fat molecules [4]. The molecules then release the energy at a frequency that is detectable by transducer for display on monitoring. A higher background fields allows for better imaging, more sensitivity and resolution of the signals. The medical field has the fastest growing demand in term of superconducting materials.

1.1.4 Power Distribution and Storage

In a world where suppliers are always attempting to limit losses, power utilities have found in superconductor based transformer a great benefit. Superconducting material with their ability to carry high current with a resistance close to null have tremendously reduces the losses for utility companies.

Energy storage is another commercial power project that employs superconductor technology to enhance power stability. This type of storage system has the ability to store over three million watts, as the D-SMES deployed in Wisconsin in 2000, and can be retrieved when there is a need to stabilize the line voltage during a disturbance in the electric grid.

1.1.5 High Speed Levitation Trains

Magnetic levitation is an area where superconductors are used in electromagnets to power high speed trains. Trains are made to "float" on strong superconducting magnets that use electrodynamic suspension (EDS), virtually eliminating friction between the train and its tracks. The EDS system uses superconducting electromagnet that creates a magnetic field, which in turn induces currents in neighboring metallic material such as the rail tracks in the case of the maglev trains. The magnetic field will be used to push or pull the train towards the design levitation position on the guide way. Conventional electromagnets waste a significant amount of electrical energy as heat and will have to be physically much larger than superconducting magnets to produce similar energy when compared to a superconducting magnet. In 2015, the MLX01 test vehicle reached a speed of 375 mph (603 km/h) breaking a land speed record for rail vehicles [6]. The wide range of applications of superconductors makes their study necessary to advance their usage in fields that are still going through the development phase.

Chapter II: Cryocooler

There is a variety of cryogenic systems that are commercially available for operation between 1.5 K and 300 K. Helium and nitrogen are typically used for cooling medium in cryogenic application. Nitrogen has a boiling point of 77 K and exists as the most abundant uncombined element. It works well for cryogenic application where the test sample can be submerged in liquid nitrogen and where temperature below 77 K is not necessary. Helium on the other hand, with its boiling point right at 4.2 K can lend itself to applications where the sample that is being tested require much lower temperature, that the case of the low temperature superconductor that are referred to in the introduction section.

In the case of our experiment, the test sample needed to remain in an environment of approximately 4.2 K. The cryocooler that was procured for the experiment is the model Special SHI-950T-15 from Janis [7], which would allow testing the sample while it is surrounded by helium gas and not submerged in a liquid.

2.1 Equipment Description

The cryocooler model SHI950T-15 is a closed cycle refrigerator system and is essentially comprised of two sections, the cold head section and the sample holder section (Figure 2). The cold head operates on a closed cycle refrigerator system knows as the Gifford McMahon cycle that will be discussed further in this thesis. The cold head has two stages with cooling capacity of 45 W and 1.5 W on the first and second stage respectively when they are at temperatures of 50 K and 4.2 K respectively. The second stage is connected by copper straps to the sample tube, where a sample can be introduced during the experiment. The refrigerator first stage cools the aluminum radiation shield that surrounds the sample tube. The test probe and sample are to be

placed in the exchange gas sample tube that in this case uses helium gas. The helium exchange gas becomes a link between the refrigerator and the sample through convection cooling. The top part of the sample tube is made out of stainless steel and the bottom is an oxygen-free high thermal conductivity copper. The walls of the bottom tube are designed slightly thicker than the top stainless steel tube above it to promote thermal stability of the system. In general, the thermal capacitance of an object provides a measure of how much energy is required to change the temperature of the object. The thermal capacitance of the object is the product of its mass and specific heat capacity. The higher the weight of an object the more capability it has to resisting a change in temperature. It might mean long cooling time, but once the target temperature is reached, the higher thermal capacity becomes beneficial.

A vacuum shroud is used to isolate the cold environment to the surrounding outside room temperature. An aluminum radiation shield surrounds the sample tube area and is cooled by the refrigerator first stage heat station. A charcoal cryopump is attached to the radiation shield and is used to remove any oil or water vapor that could be present in that space. The presence of oil or humidity can negatively affect the efficiency of the system (Figure 25)

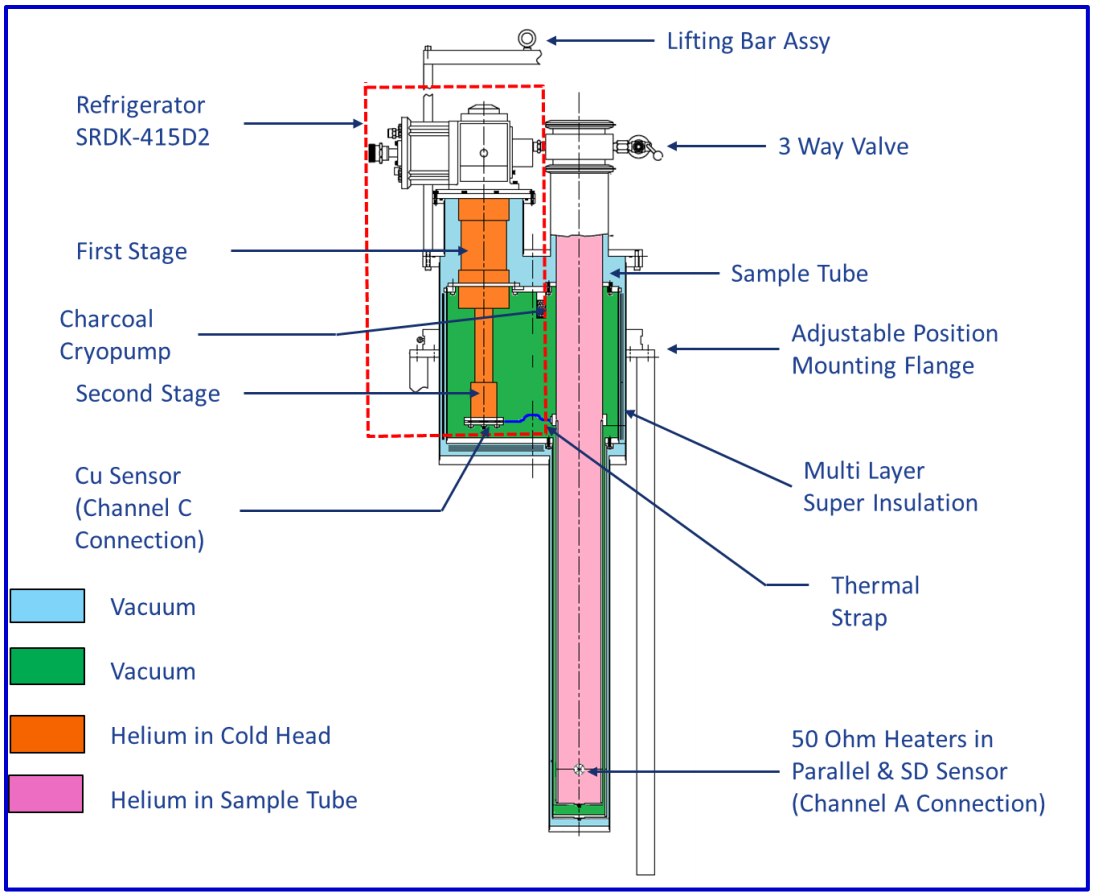

Figure 2. SHI-950T-15 Cryostat with sample in exchange gas [7]

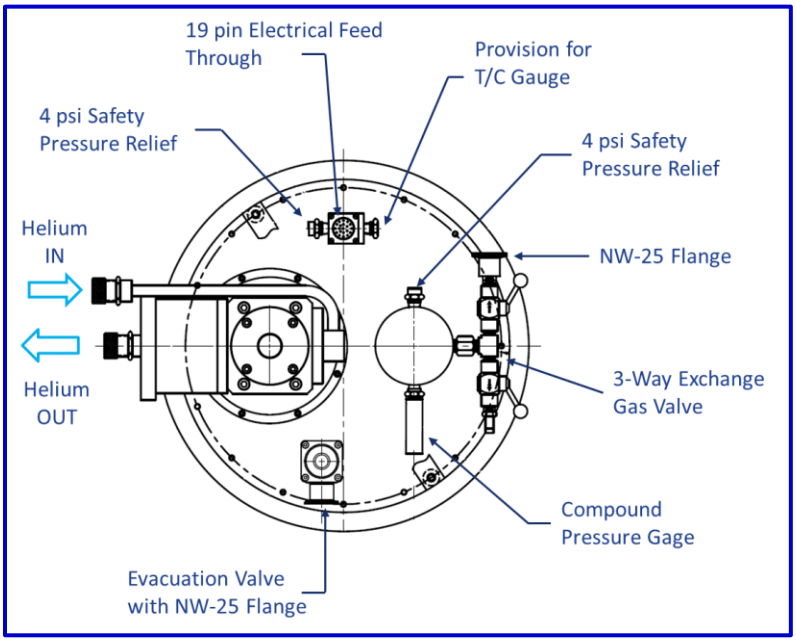

Figure 3. Cryostat top view of cryostat [7]

2.2 Gifford McMahon Cycle Principle

The Gifford- McMahon refrigeration cycle was first introduced in 1959 and has found widespread applications in many low temperature systems such as MRI and cryopumps. The cold head has mainly three parts that consist of the compression and expansion space, the regenerator and the displacer. The high pressure helium from the compressor enters the cold head through the hose connector that bridges between the compressor and the cold head. The Gifford McMahon cycle uses gas regenerator to permit cooling to cryogenic temperatures. The regenerator can cool gases to a temperature of 4.2 K due to the special rare earth material it is made with. The regenerator is usually made from materials that have poor thermal conductivity, high specific heat and large surface area. With such characteristic, the regenerator is able to capture the heat from the incoming helium gas, and is able to give up the heat to the colder exiting helium gas.

Inside the GM cooler are inlets and exhaust valves in the cold head that are actuated by a rotary mechanism (rotating valve) and the displacer is driven either pneumatically or by the synchronous motor that drives the valves. The helium gas expansion in the displacer-regenerator assembly provides the cooling for the first and second stage heat stations.

The cold head consists of two cylinders, one for the first stage and one for the second stage where each stage has its own displacer. The cold head also has a drive mechanism and drive motor as described above. The first stage displacer connects to a scotch yoke, which is driven by the motor through a crank and bushing. This mechanism converts the rotating motion of the motor to a translational motion for the displacer. The crank also drives a rotary valve which

controls the timing of the helium gas intake and exhaust, that is synchronized with the reciprocating motion of the displacer assembly.

The displacer assembly consists of the regenerator which slide within the cylinder, it allows the helium gas to pass through it, and creates the cooling of the gas. The pressure above and below the displacer is quasi balanced except for a small pressure drop across the regenerator that occurs when helium is passing through it. There is no work being done on the gas and the gas does not work on the displacer. It requires very minimal work to move the displacer within the cold head cylinders. The inlet and outlet valves control the pressure in the system by either increasing or decreasing it depending on the need.

The cycles for the GM refrigerator can be divided into four steps, with Fig. 4 as follow:

The cycle starts with the low pressure valve closed, the high pressure valve open and the displacer is moved all the way to the left as shown in fig 4. It is to be noted that the cold head in our application is upright and therefore the left and right of the schematic representation in figure 4 corresponds to respectively down and up position of the displacer.

a. The next step in the cycle consists of moving the displacer to the upper level inside the cylinder while the cold head is connected to the high pressure valve of the compressor. The motion of the displacer to this new position will force the gas in the cylinder to pass through it. The gas initially at the compressor exit temperature passes through the regenerator and leaves with much colder temperature. Heat is released to the regenerator material in the process.
b. In the next step, the high pressure valve is closed and the low pressure valve is opened with the displacer all the way at the top of the cold head cylinder. Because of the depression that

occurs as a result of the low pressure being opened, part of the gas flows through the regenerator to the low pressure side of the compressor. That is the most important step as the gas expands, this is where the useful cooling power is produced. The expansion is isothermal, so heat is taken up from the cooling space.

c. In the following step, the displacer is moved completely to the bottom with the cold head connected to the low pressure side of the compressor forcing the cold helium to pass the regenerator. Some heat will be taken by the regenerator during this process.
d. In the last step, the low pressure valve is closed and the high pressure valve is opened with the displacer remaining at the bottom of the cold cylinder head. The gas trapped in the hot side of the cold head is now compressed as a result and heat is released to the surroundings.

The frequency of the motor and displacer movement in the GM cooler is about 2 Hz to 3 Hz and is uncoupled with the compressor, so that each can run independent of the other.

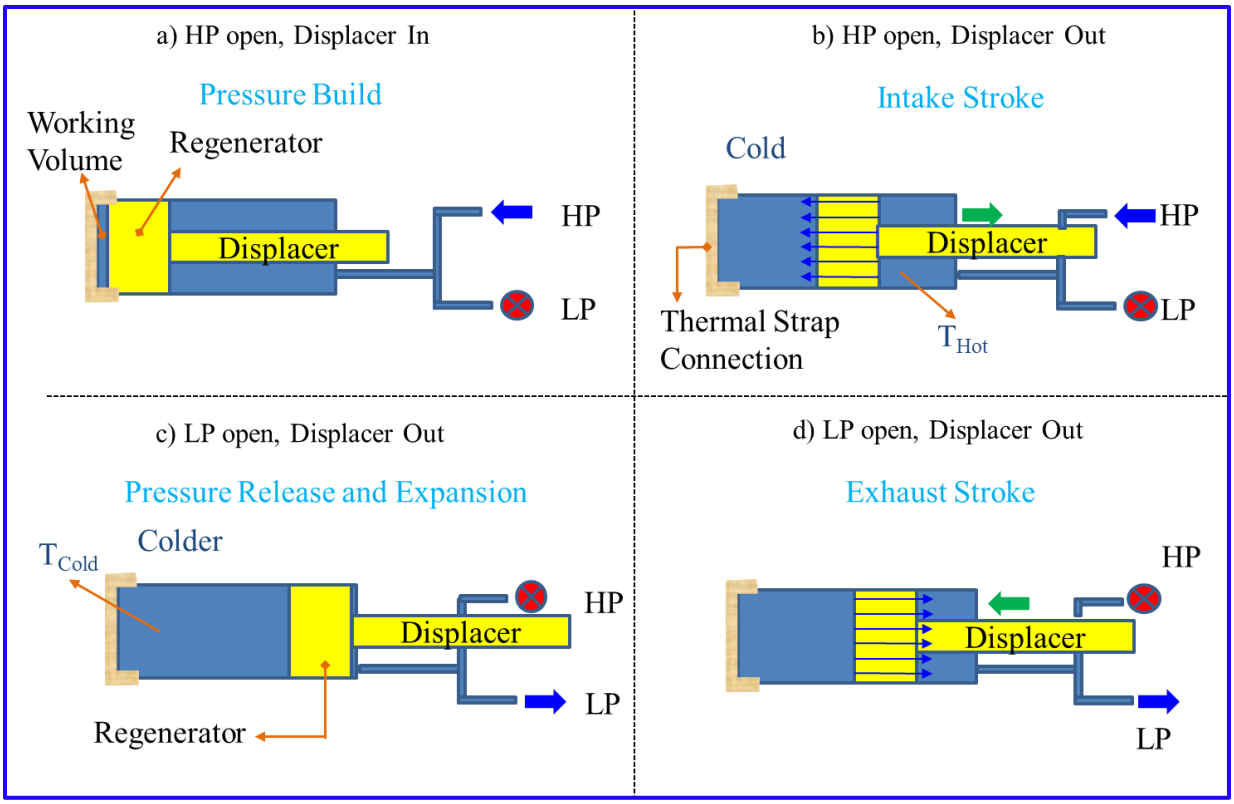

Figure 44. Gifford McMahon cycle description [8]

2.3 Test Setup

2.3.1 Operating the Equipment

The system requires special care to avoid hazardous condition during the system operation. Cryogens can be dangerous if handled improperly. Typically, cryogenic liquid are those defined as liquid with a normal boiling point 123 K. In the case of the special SHI-950T-15 Cryostat helium with a boiling point of 4.2 K is used as the cryogenic fluid. The important factor is that, it has an expansion ratio of about 750. With such a high expansion ratio, it can result in high pressures that may cause an explosion. Because the temperature of the cryostat has to reach very low temperature the presence of water or air molecule inside the system can be detrimental. All precautions must be taken to prevent water from getting into the cryostat and insuring that any

air inside is removed from the cryostat before running the experiment at cryogenic temperatures. Water in the air can also freeze and form a blockage inside the system, trapping liquefied air below that is waiting to create an explosion. When liquefied air boils at 81.6 K, the pressure build inside the cryostat can cause an explosion. While the system is operating, one shall stand clear from the system and avoid exposing one's body directly above the sample zone.

The special SHI-950T-15 refrigerator cold head should be set upright for highest efficiency. Other orientation can decrease the efficiency by as much as 15% which would prevent from achieving satisfactory minimum temperatures. A separate compressor assembly which must also stand upright at all times is required to circulate the helium to the cold head. The details on the compressor are covered later in this thesis.

A sample can be loaded from the top of the cryostat and supporter at the top by the flanges of the test probe. Based on the ice build-up and air trapped risk mentioned above, the system must undergo an evacuation to remove the air from the interior of the cryostat. The special SHI-950T-15 is equipped with bellows seal evacuation valve which allows evacuation and sealing of the insulation vacuum jacket. The space surrounded by the aluminum shroud must be vacuumed prior to cool down to a pressure of 1e-5 Torr (.001 Pa 1.9e-7 psi) or less, using the evacuation valve shown in figure 3. Better vacuum levels provide greater insulation, resulting in shorter cool down times and lower final temperatures. A turbomelocular pump model TS75D1002 from Edwards Limited [9] is used to vacuum the aluminum shroud. The evacuation valve shall be firmly sealed once the vacuum process is complete. The evacuation process is to be initiated whenever the minimum temperature begins to increase after the system has reached a steady

state operating condition. This is necessary because outgassing and O-ring leaks will cause the pressure to rise slowly overtime while the system is operating.

One of the connections on the three way exchange gas valve located near the top of the sample tube is used to first evacuate the sample tube to a pressure of about 1e-3 Torr (.133 Pa or 1.9e-5 psi) in order to reduce the risk of air being present inside the sample tube. The other open end of the three way valve can be used to supply helium gas to the sample tube once the air vacuum side is closed. The helium valve is closed once the 4 psi safety pressure relief valve begins venting.

It is to be noted that the exchange gas valve and the clamp on the top port of the sample tube must be properly closed before starting the system otherwise there is a potential risk for the formation of hazardous ice blockages.

Before the cool down can be initiated, the automatic temperature controller is switched to the ON setting. The temperature controller is a lakeshore two channel temperature This temperature controller is connected to the sensor located almost at the lower end of the sample tube as shown in figure 2. It will therefore allow a reading of the temperatures on the sample tube. The temperature readings will be somewhat close to room temperature when the system is first turned on.

The compressor is then turned on and the cold head will start cooling down almost immediately. It usually takes about four to six hours to reach a base temperature of 4.2 K at the bottom of the sample tube. For the cryostat to reach the lowest temperature specified by the supplier, the amount of exchange gas in the sample tube might require some adjustment by adding some helium since cooling the helium will cause the pressure to decrease following the ideal gas law.

The temperature controller can be used to control the temperature in the operating range of 4.2 K to 300 K. The 50 Ω heater installed on the sample tube as shown in figure 2 is used as a control for maintaining the temperature to the level that is needed. The two possible modes of operation of the system are, exchange gas control, dual channel control.

When the exchange gas control option is chosen, the controller heater output connectors are connected to the electrical feedthrough situated at the vacuum jacket top flange. The temperature in the cryostat is raised by the increase of the temperature of the heater, which indirectly heats up, by convection, the helium in the sample tube. The advantage of this method is that the temperature around the sample will remain more uniform, since the sample is surrounded by isothermal gas.

The dual channel controller provides the controlled environment with the use of a loop. The main heater loop is connected to the sample tube heater and the secondary loop is connected to the second stage. This method not only provides even more uniform temperature at the bottom of the cryostat, the temperature will stabilize rather shortly compared to the exchange gas control method.

2.3.2 Procedure for Shutting Down

The pressure inside the cryostat is below atmospheric during normal operation of the cryocooler; the pressure is therefore increased by introducing helium from the helium tank, otherwise directly opening the sample tube to the atmosphere could cause severe damage or injuries. The pressure is increased until it vents through the safety pressure relief valve. The top cap V-band clamp is then removed to allow for the sample to come out. The top cap is to be replaced immediately to prevent air and moisture from entering and freezing with the cryostat.

The system is shut down by simply turning off the compressor and the temperature controller. In the event that a fast warm up is needed, heat can be applied to the sample tube, to bring the temperature to room temperature again. It is recommended not to exceed 300 K otherwise damages to the heater and thermometer may occur. It is also recommended not to remove the interconnecting gas line until the temperature in the cryostat has completely stabilized with the surroundings room temperature, if there is a need.

The SHI-950T-15 allows for cooling a sample to low temperature without coming in contact with the helium gas, reducing the risks involved, however caution must be exerted all the time while working with the equipment because of all the reason that were discussed previously.

Chapter III: Compressor & Water Chiller Description

3.1 Compressor Description

The compressor that was used for the experiment is a helium compressor model F-70L from Sumitomo Cryogenics of America Inc. The compressor provides high-pressure oil free helium gas with 99.999% purity to the cold head of the cryostat. The compressor also supplies the power to the cryostat, it is therefore necessary to first turn on the compressor in order to get the cryostat operating. Self-sealing gas line couplings are used to connect to the cryogenic refrigerator RDK-415D cold head.

The role of the compressor is to continuously circulate helium in the system by drawing low pressure helium compressing it, cooling and cleaning the helium from oil that the compressor needs to operate before the helium is returned to the cold head at high pressure.

The helium gas exits the compressor capsule with heat that needs to be removed and compressor lubricant. The hot gas is taken to an oil separator that operates on the principle of gravity. Inside the cavity of the oil separator, the gas mixture finds a spinning mechanism, which by centrifugal force - as the air spins inside the cavity, the oil drops out because the oil particles are heavier than the air particles, they accumulate on the wheel and they get pushed out while the gas carries out the circuit. Next, in order to remove the heat, the gas is directed to a heat exchanger where it is cooled. The gas then goes through another oil separator and moisture removal, which removes oil in the system furthermore more. By cooling the gas, part of the oil present in the gas will condensate therefore making it possible to be extract from the flow. The absorber removes all remaining oil before the helium gas makes it way to the cold head. From that point, the high pressure helium has a purity of 99.999% and is directed through the high pressure gas line to the

cold head to be used for cooling the cryostat. There are mainly two gas line connecting the compressor and the cold head. One carries low pressure helium gas back to the compressor and the other one carries high pressure helium gas to the cold head. The oil collected from the oil separator is returned to the compressor capsule through capillary tubes and orifices, while any oil removed in the absorber will remain inside until the compressor is overhauled and the absorber requires some maintenance. The oil removed from the first oil separator, is cooled in the heat exchanger and returned to the compressor capsule to absorb heat from the low pressure side and to lubricate the compressor capsule.

Inside the compressor, an internal relief valve is positioned in parallel between the low pressure and high pressure gas line to prevent overloading the motor when the system gas lines are not connected to the compressor. Figure 5 provides the schematic of the compressor.

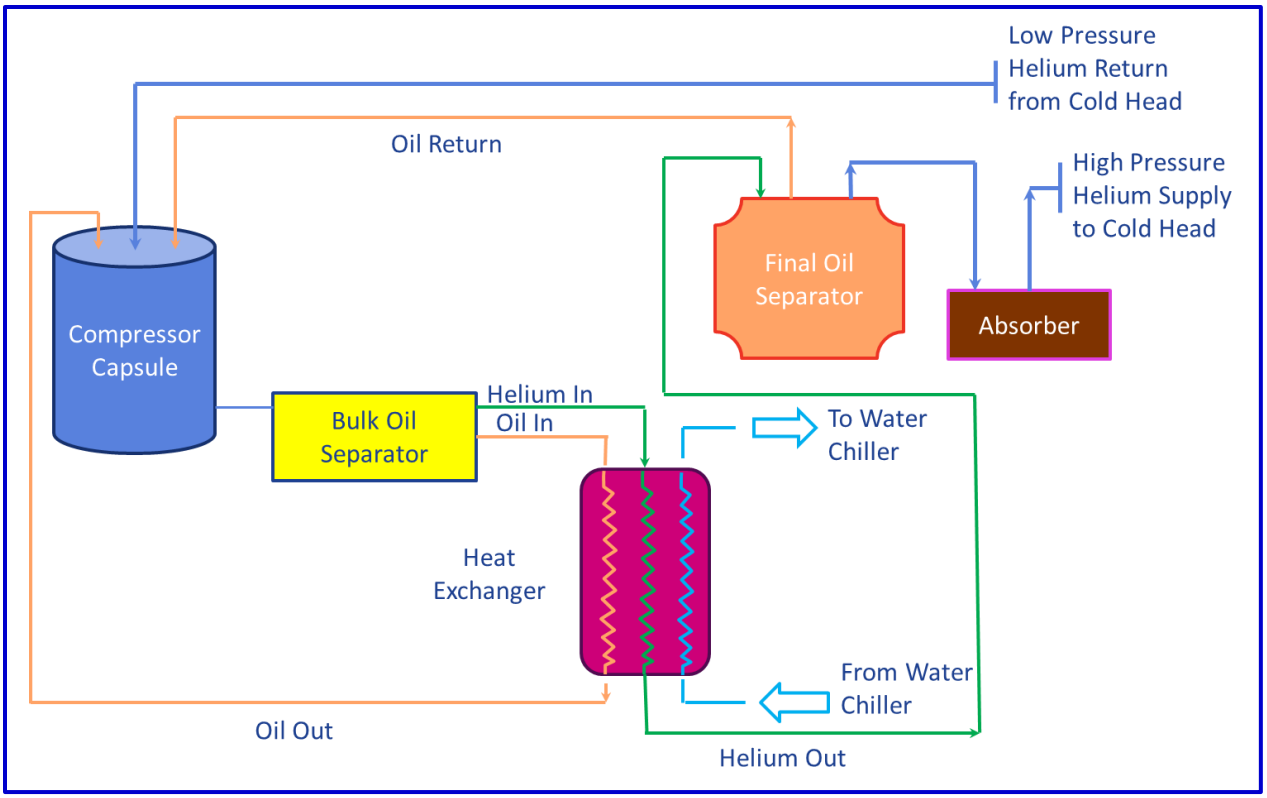

Figure 5.5 Compressor F70L principle [10]

3.2 Water Chiller Description

At a certain point in the cycles of the compressor, the helium gas requires some cooling before it is returned to the cold heads, a chiller was used to that effect. The chiller model used for cooling the helium circulating in the compressor is a 3-Ton Water Chiller made by Dimplex Thermal Solutions Company, model SVI-3000-M figure 6.

Figure 66. SVI3000M Dimplex Solution 3 Ton Water Chiller [11]

The water chiller operates in a close loop where water is circulated between the compressor and the chiller to remove the heat from the helium gas and to reject it to the atmosphere. There are two circulations inside the water chiller, one that circulates water/glycol from and to the compressor and the second circuit is a refrigeration cycle that provides the cooling capacity to the chiller. The water/glycol mixture circulates between the heat exchanger in the compressor and the water chiller. Hot water/glycol mixture leaves the compressor where heat is removed from the helium gas and transferred to the water/glycol mixture by the mean of a heat exchanger. A pump inside the chillier allows the continuous circulation of the water. Inside the chiller, the hot water/glycol goes through another heat exchanger where heat is removed from the water and transferred to a working fluid that circulates inside the refrigeration cycle. The refrigeration system of the chiller uses a close loop circuit in which the working fluid is a hydrofluorocarbons called R-407C. The refrigeration system has mainly four components: a compressor, a condenser, a thermostatic expansion valve and an evaporator as shown in figure 8.

The compressor main goal is to raise the pressure of the refrigerant vapor to a level high enough such that it can be condensed. The compressor also provides the pumping mechanism for the system. After the gas leaves the compressor, it goes into the condenser where heat absorbed by the refrigerant is given off to the surrounding air by mean of a heat exchanger. The heat exchanger is cooled using a forces convection mechanism where a fan blows air on the condenser to expel the heat to the surroundings. The temperature of the high pressure vapor drops, therefore allowing for condensation to liquid.

The liquid refrigerant is then taken through an expansion valve where the cooling takes place. The refrigerant temperature drops significantly and becomes a mist at that point as it makes its way into the evaporator. In the evaporator the refrigerant boils, turning into mostly gas, absorbing heat as it evaporates and cooling the water/glycol mixture that flow in the heat exchanger. The compressors cooling requirement is that the water/glycol mixture entering the compressor has a temperature range between 5^{o} C to 25^{o} C.

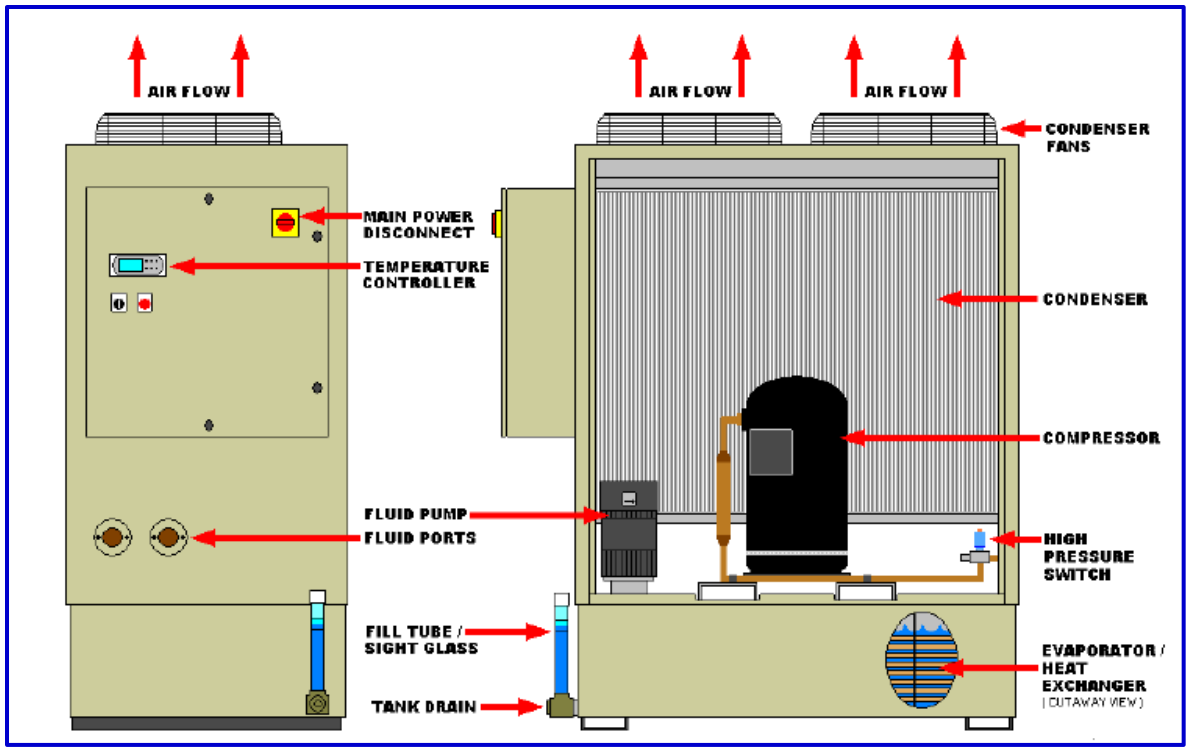

Figure7 7. Water chiller components [11]

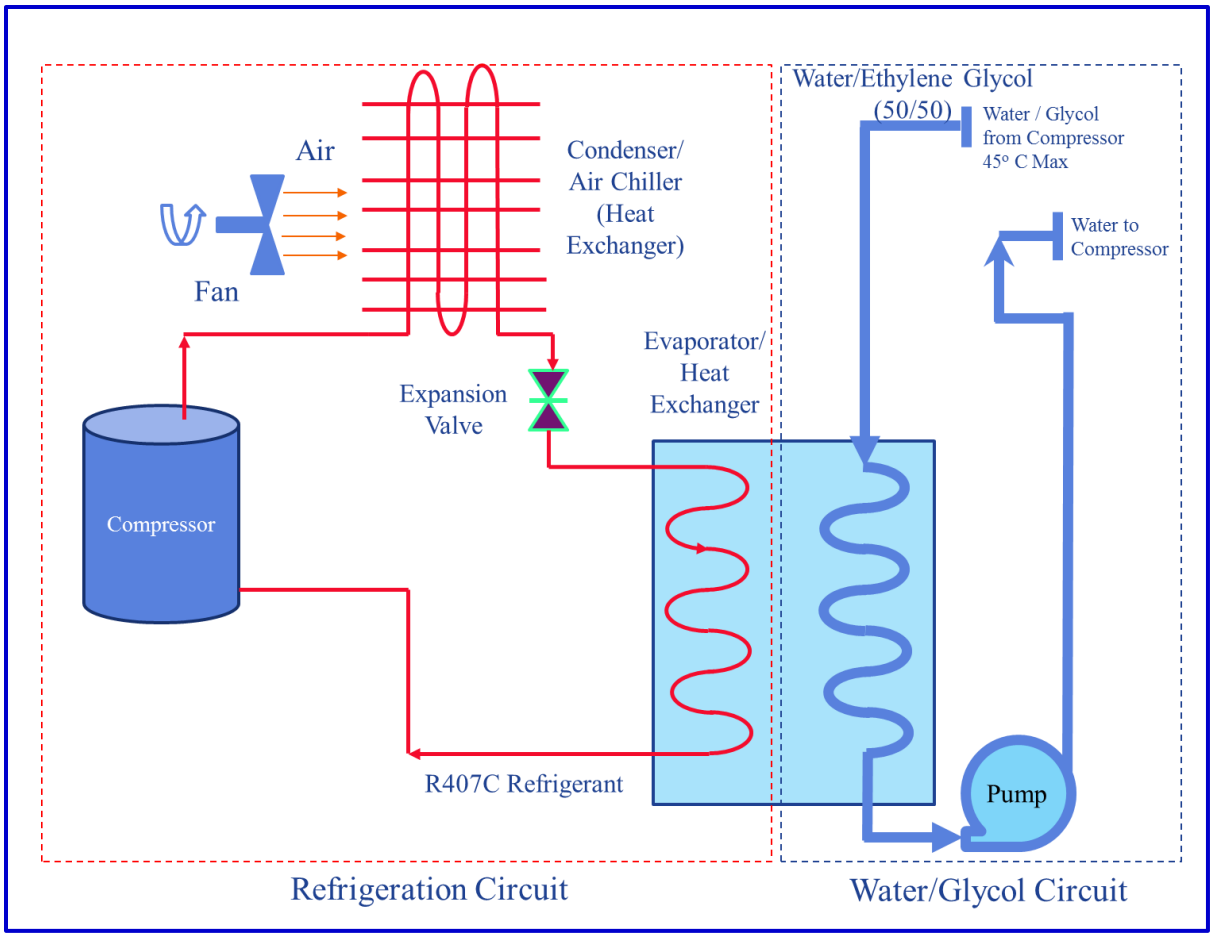

Figure 8. Water (50% water, 50% glycol) chiller operating principle [11]

Chapter IV: Heat Transfer Study

Heat transfer is the most important factor for a cryogenic experiment as material superconductivity in part is a function of temperature. For the experiment to be successful, the heat flow to and from the sample area has to be estimated accurately. Heat transfer takes place in three forms depending on the medium; conduction, convection and radiation. The other factor that is to be accounted in the heat transfer study is the heat source, which in the case of our experiment, is heat through conduction from hardware extending outside the cryostat to room temperature and joule heating. Joule heating also known as resistive heating comes in the form of heat generated from the current that is travelling in the electrical wires. It is function of the conductor resistivity. Superconductors have zero resistivity therefore does not produce joule heating. The purpose of this chapter is to therefore study the temperature distribution in the sample tube using the finite element analysis tool ANSYS® Fluent.

4.1 Analytical Approach

The analysis of the sample tube environment that is filled with helium gas was the first step in the process of estimating the ongoing heat transfer. Convection cooling is the primary method used inside the cryostat to keep the temperature of the sample close to 4.2 K. The connection between the cold head and the sample space and the effectiveness of the thermal insulation from the outside environment are key factor that influence the cooling efficiency of the system.

The maximum cooling capacity of the Cryocooler (figure 9) dictates how much cooling can be provided to the system. The cooling capacity is a function of temperature and decreases with decreasing temperature.

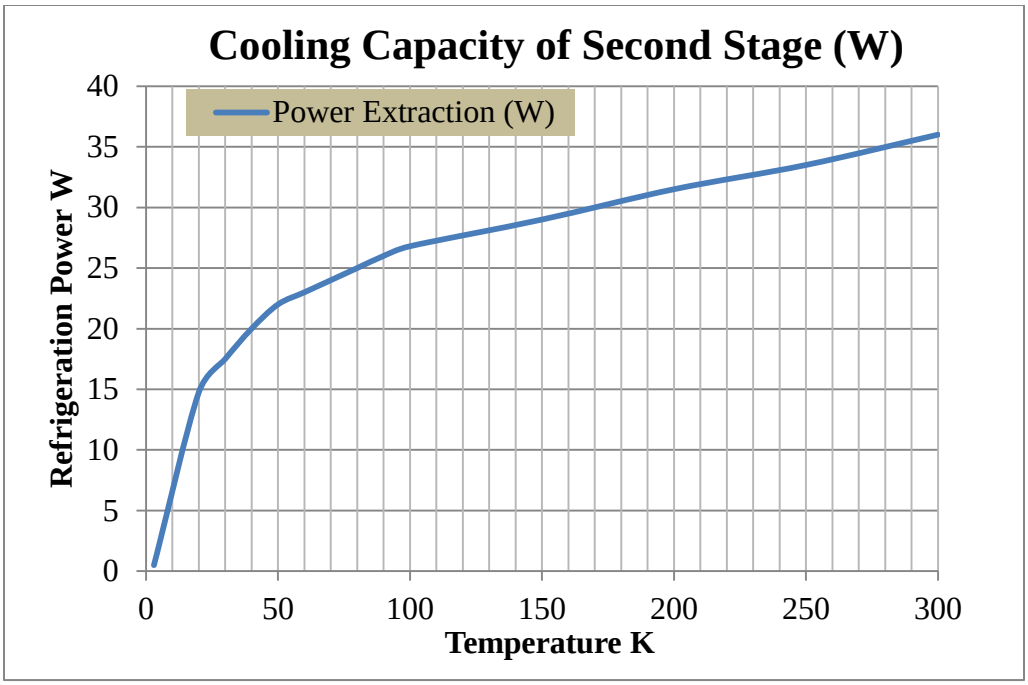

Figure 99. Approximate cooling capacity of second stage [7]

The heat capacity of the sample and test rig devices also affects the cooling efficiency. The thermal resistance as it was previously defined is directly related to the mass of the material and its specific heat capacity. The more mass is introduced into the sample tube, the less efficient the cooling. Also material with high specific heat capacity will yield poor efficiency in cooling. Material such as fiberglass G10 will typically offer low density and low specific heat capacity that makes it a good candidate if the sample is not to be tested for strength and only current carrying capability is what is being investigated.

The thermal insulation is the other factor that can influence the efficiency of the system. In our case, the sample was isolated from the room temperature environment by means of two vacuumed chambers; the cold heads have in addition to these, a radiation shield.

The quality of the connection between the cooled parts and the cold head also influences the cooling efficiency. In the case of the Cryocooler Special SHI-950T-15 cryostat, the cold head is connected to the sample tube via a thermal strap, which in turn cools the sample tube by conduction. The sample tube then cools the helium gas within its cavity through conduction and convection. The free convection that takes place within the sample tube is very negligible. In Free convection, the fluid motion is due to buoyancy forces within the fluid which allow for cold gas to sink and a hot gas to rise. It is important to note that buoyancy is due to the presence of a fluid density gradient and body force that is proportional to density. The body force is gravitational and the fluid density gradient is driven by temperature gradient inside the controlled volume. The Cryocooler in the lab is setup to stand in the upright position where the top end of the sample tube is capped by a fiber glass G10 plate where all the wiring feed through to the inside of the sample tube. The bottom of the sample tube is insulated by two layers of vacuumed cavities making it colder at the bottom than at the top. The hot gas therefore remains at the top with nowhere to go and the cold gas trapped at the bottom of the sample tube. The cooling of the sample tube and test rig hardware placed in the sample tube is mainly through convection which can be considered as a combination of thermal conductivity of the gas and the dynamic movement of its particles. The dynamic movement of the particle is very limited because of the Cryocooler setup does not exactly promote free convection. The other factor that lead to poor free convection is the pressure level that the system gets to once the temperature is lowered to cryogenic temperature. At low pressure, there is an increase in the mean free path of gas molecules which reduces heat transfer by convection of the helium gas.

4.2 Heat Transfer Approximation

The objective of this section is to develop a model that is accurately portraying the temperature profile of the sample tube control volume inside the cryocooler. Conduction, convection and radiations are the means of heat transfer methods that apply to control volume of the cryocooler. Considering the control volume surrounding the sample tube a conservation of energy equation can be written in the form of:

$$Q_{in} + Q_{gen} - Q_{out} = Q_{Stored} \qquad (1)$$

Where:

- Q_{in} is heat coming into the system from outside in the form of radiation and conduction from the sample tube top cover.

- Q_{gen} is the heat generated inside the control volume in the form of joule heating. For now there is none, since we are assuming that the sample tube is empty. This will become an important factor when the electrical wires are introduced later for the test and they produce heat as a result of current flowing inside.

- Q_{out} is heat removed from the system mainly through conduction and convection.

- Q_{stored} is heat stored inside the control volume. No energy is stored in the control volume here.

This equation can be rewritten in the form:

$$\boldsymbol{Q_{cond} + Q_{conv} = Q_{rad}} \qquad (2)$$

Or more explicitly:

$$\boldsymbol{\nabla}.(\boldsymbol{k} * \boldsymbol{\nabla} * \boldsymbol{T}) + h * (T_s - T) = \boldsymbol{\varepsilon} * \boldsymbol{\sigma} * [(\boldsymbol{T_{s1}})^{\boldsymbol{4}} - (\boldsymbol{T_{s2}})^{\boldsymbol{4}}] \qquad (3)$$

Where:

- k is the thermal conductivity.
- T is the temperature of the fluid.
- h, is the heat transfer coefficient of the fluid.
- T_s is the temperature at the surface of the sample tube
- T_{s1} and T_{s2} are the surface temperature of the sample tube wall facing each other
- ε is the emissivity coefficient and is function of the material and it surface finish.
- σ is the Stefan-Boltzann constant [5.67×10^{-8} W/(m^2K^4)].

Convection is based on the Newton's law of cooling where the convection coefficient is function of conditions in the boundary layer, which are influenced by surface geometry, the nature of the fluid motion, and several fluid and thermodynamic properties. The convection coefficient is generally given as:

$$h = \frac{L}{K} * Nu(Ra, Pr, Re) \qquad (4)$$

Where L is the characteristic length; the Nusselt, Raleigh, Prandtl and Reynolds numbers are characteristic dimensionless values. The phenomenon of the natural convection was not taken into account in the ANSYS FLUENT ® simulation as it became clear that free convection does not play a role in the heat transfer process. As discussed in reference 15, an unstable temperature gradient would allow for free convection however, a stable temperature gradient, which we have in the case of our Cryocooler; the heat transfer takes place by conduction.

4.3 Finite Element Models and Boundary Conditions

The model geometry was imported into ANSYS® from Unigraphics® [23]. In the first step, the model included only the solid element of the Cryocooler to try and determine the effect of conduction and radiation on the system if no helium is present (Figure. 10). The helium in the sample tube serves as a link between the sample tube and test rig equipment to provide the cooling necessary. The boundary conditions are setup to best reflect the constraints on the actual Cryocooler from observation that was made on the equipment in the lab. The lateral and bottom surface of the outer stainless steel shell that contained the cold heads are modeled as insulated surface. The top part of that shell was set to have room temperature. A temperature boundary condition was established at the contact between the first stage and the aluminum shroud, since it is known based on the instructor manual that the first stage is used in cooling the shroud. Three boundary conditions with surface to surface radiation are set for the internal cavity of the sample tube and aluminum shield that surrounds it. Another radiation boundary is placed between the aluminum shield and the outer stainless steel layer. The value for the emissity is as specified in reference for the respective materials that make out the different parts. A temperature boundary condition of 300 K and 4.2 K are respectively placed at the top of the G10 cover plate and the contact area of the thermal strap.

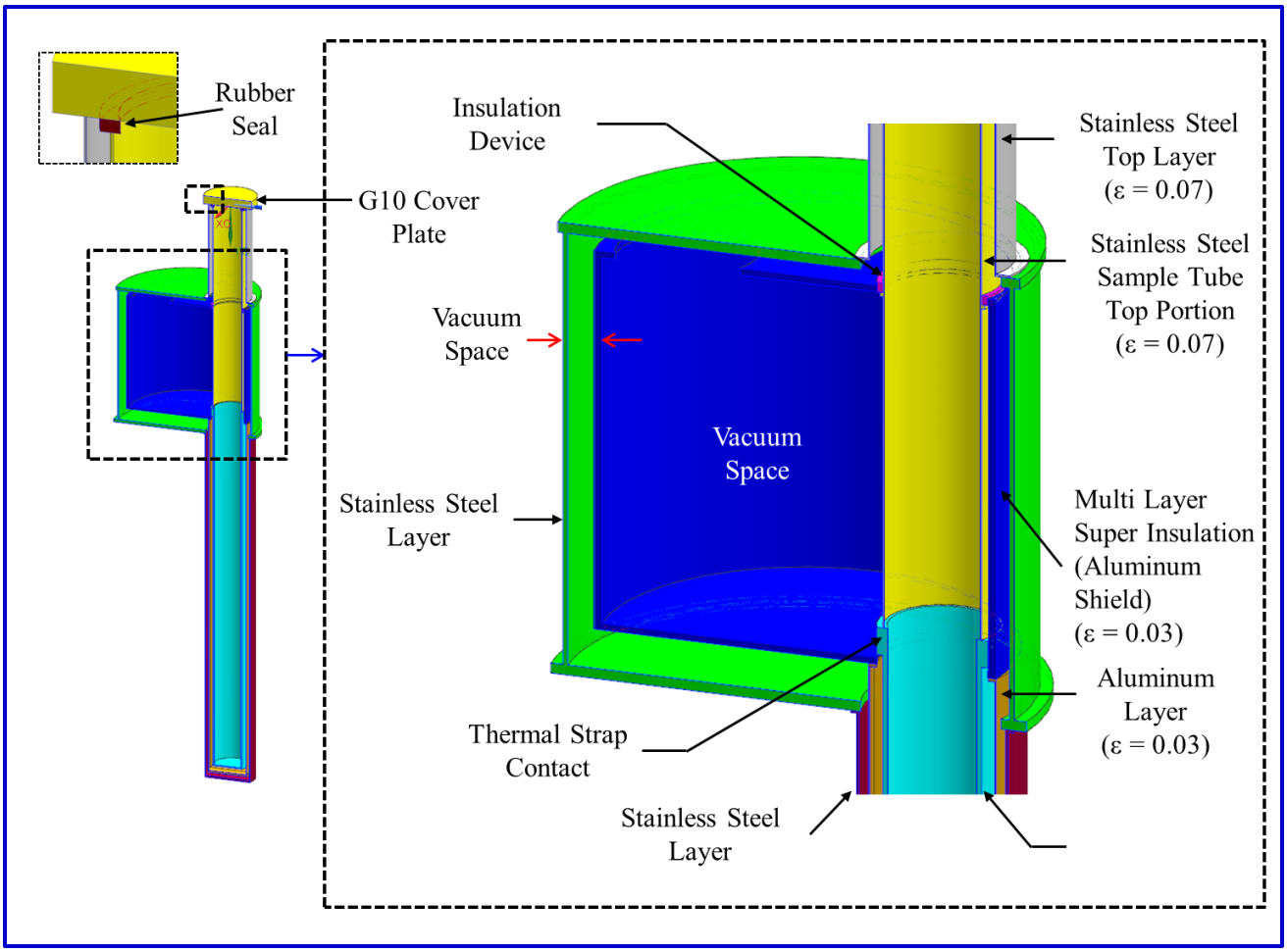

Figure 1010. Heat transfer solid model [7] [18]

In the second part of the simulation, the heat transfer study focuses on determining the temperature profile of the helium inside the sample tube. The model for this case only included the sample tube and fiber glass G10 top cap in addition to the fluid (Fig. 11). We arrived to this approximation after obtaining the temperature distribution of the solid model. It suggested that an insulated boundary condition could be applied on the outside surface of the sample tube. The thermal strap connection to the sample tube is represented with a half hallow cylinder integrally

connected to the sample tube. This representation is an approximation of what the interface is believed to be based on the diagram that was supplied by the cryocooler manufacturer.

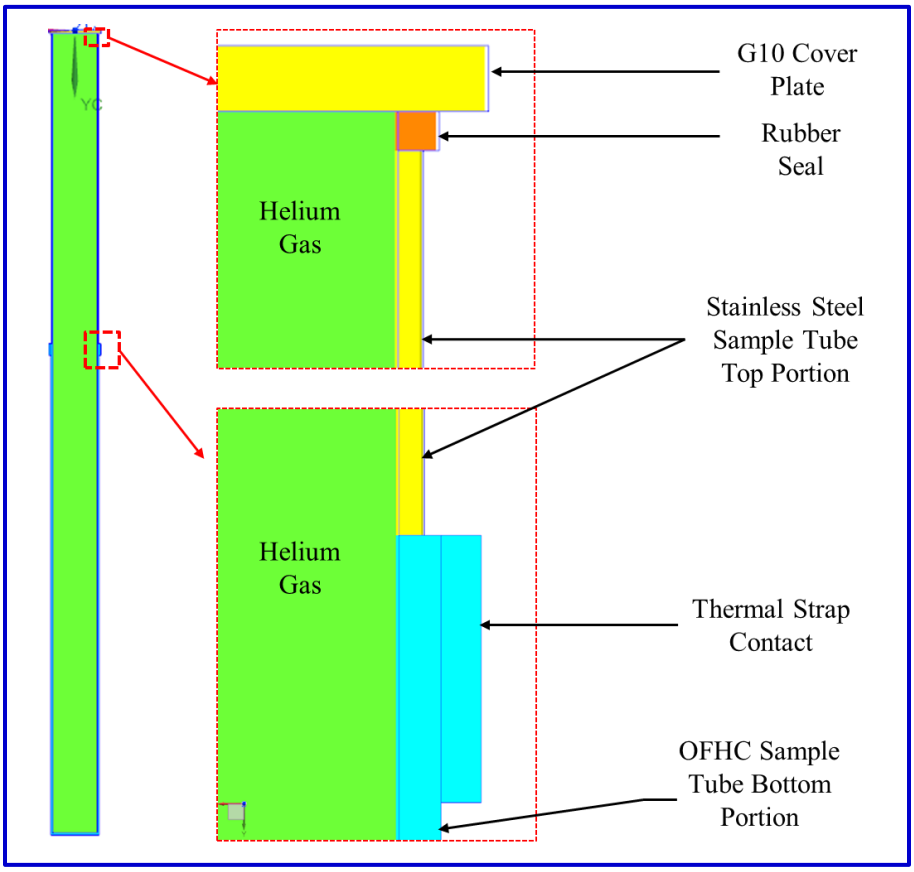

Figure 1111. Fluent model [7]

The boundary condition consists of maintaining a constant temperature of 300 K at the top surface of the G10 cover plate and a temperature of 4.2 K at the interface of the thermal strap. The rest of the external surfaces are insulated. The solid thermal model as the results showed that the layer of vacuum and radiation shielding is effective and it can be assumed that all the external surfaces of the sample tube can be treated as insulated. The helium gas is coupled to the internal faces of the sample tube. Through conduction the helium get cooled, which can be a very

slow process as the conduction coefficient of helium is very low. Gases in general have a very low conduction coefficient when compared to solids [16]. The surface to surface radiation is also computed for this model where the internal faces of the sample tube transmit heat to each other. The model is solved using the pressure based solver within ANSYS Fluent®. The free convection feature was not activated for this simulation as it was justified previously that conduction was the driving mechanism of heat transfer. The material properties were tabulated as a function of temperature. It required assuming that helium behaved as an ideal gas to reach a reasonable solution.

The fluent model is used to further analyze the temperature in the sample area, by introducing a rod that measured 1.35 meters in length, extending from room temperature at the top cover, to the bottom of the sample tube. The goal of this analysis was to determine the temperature distribution inside the sample tube to verify an experiment that was conducted in the lab. The experiment [28] consisted of introducing a copper rod inside the sample tube and measuring the temperature at the bottom of the rod. The temperature measurement of the thermocouple recorded approximately 35 K. Here, the free convection effect is taken into account because the condition of an unstable gradient is very likely. Heat transfer trough conduction by the copper rod could drive a temperature rise in the lower portion of the sample tube, therefore creating a favorable environment for free convection. The same simulation is repeated where the rod is given G10 fiberglass material properties to determine the role conductivity might play in allowing us to reach the lowest temperature possible.

To summarize, there were four models used to study the temperature distribution in this section:

- A solid model of the entire cryocooler to determine the temperature distribution of the metal

- A fluent model of the sample tube containing helium to establish the temperature distribution of helium gas inside sample tube when only helium is in the sample tube.
- A fluent model of the sample tube containing helium and an OFHC copper rod to highlight the importance of the conductivity of a material introduced in the cryocooler and the effect it could have on the temperature distribution.
- A fluent model of the sample tube containing helium and a G10 rod to highlight the importance of the conductivity of material introduced in the cryocooler and the importance of selecting a material with low conductivity.

4.4 Finite Element Mesh

The model was meshed using quad mesh elements since the geometry allows for this type of element (Figure 11). Brick elements are generally recommended for a computational efficiency. The mesh size is setup to be 2 cm on each side of the brick element. A total of 21,305 elements with 83,468 nodes are used by the model. Solid heat transfer modeling does not generally require high mesh density to provide accurate results, increasing the mesh density to a finer mesh will not make much difference in the results obtained [21].

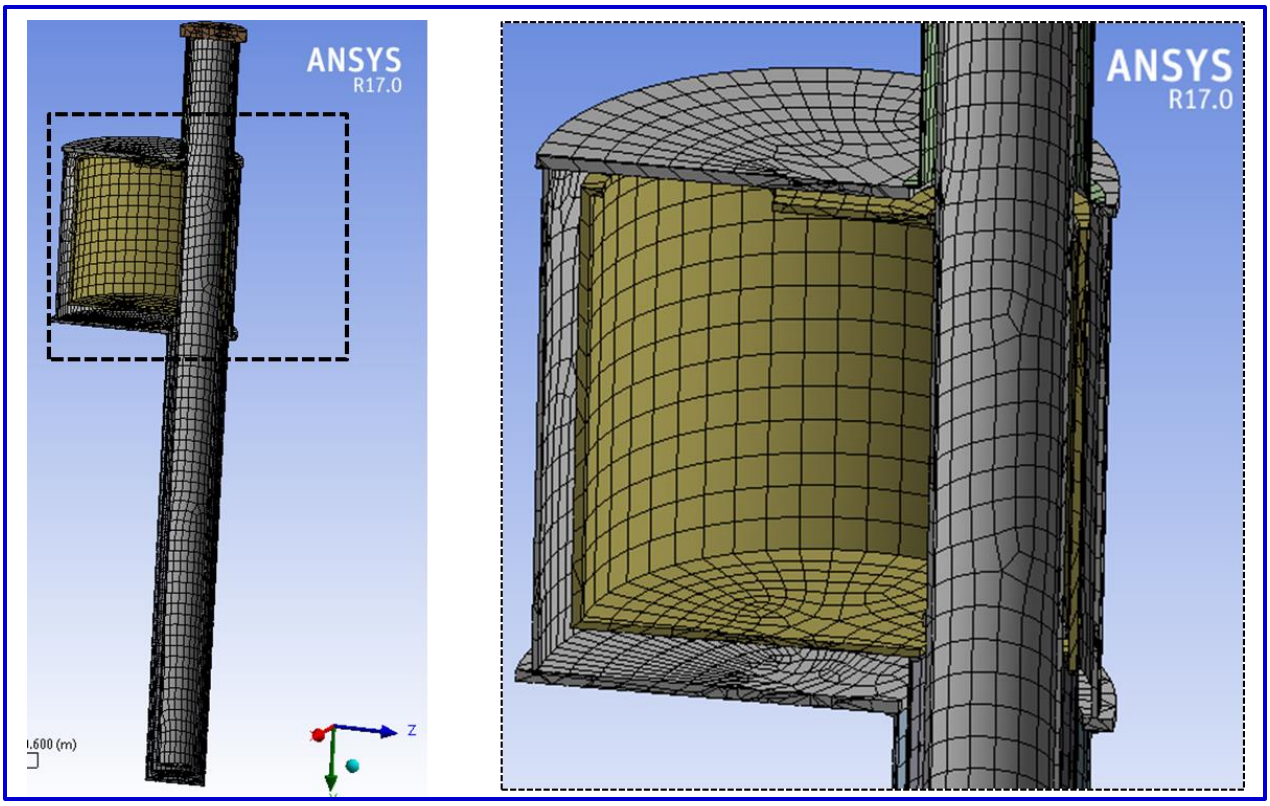

Figure 1212. Solid model mesh [7]

The ANSYS Fluent® model requires a finer mesh to be able to capture all the details of the physics inside the helium gas, therefore the mesh size is set to be ten time finer than the solid model case. The mesh here used a combination of tetrahedron and brick elements where the model allowed for that (Figure 13). Usually sweepable geometry allows placing brick elements in a specific geometry, and that is the case for most part in the model. The model is meshed with a total of 1,228,961 elements with 3,735,567 nodes. The properties for the different elements were obtained from different source and can all be found in the appendix.

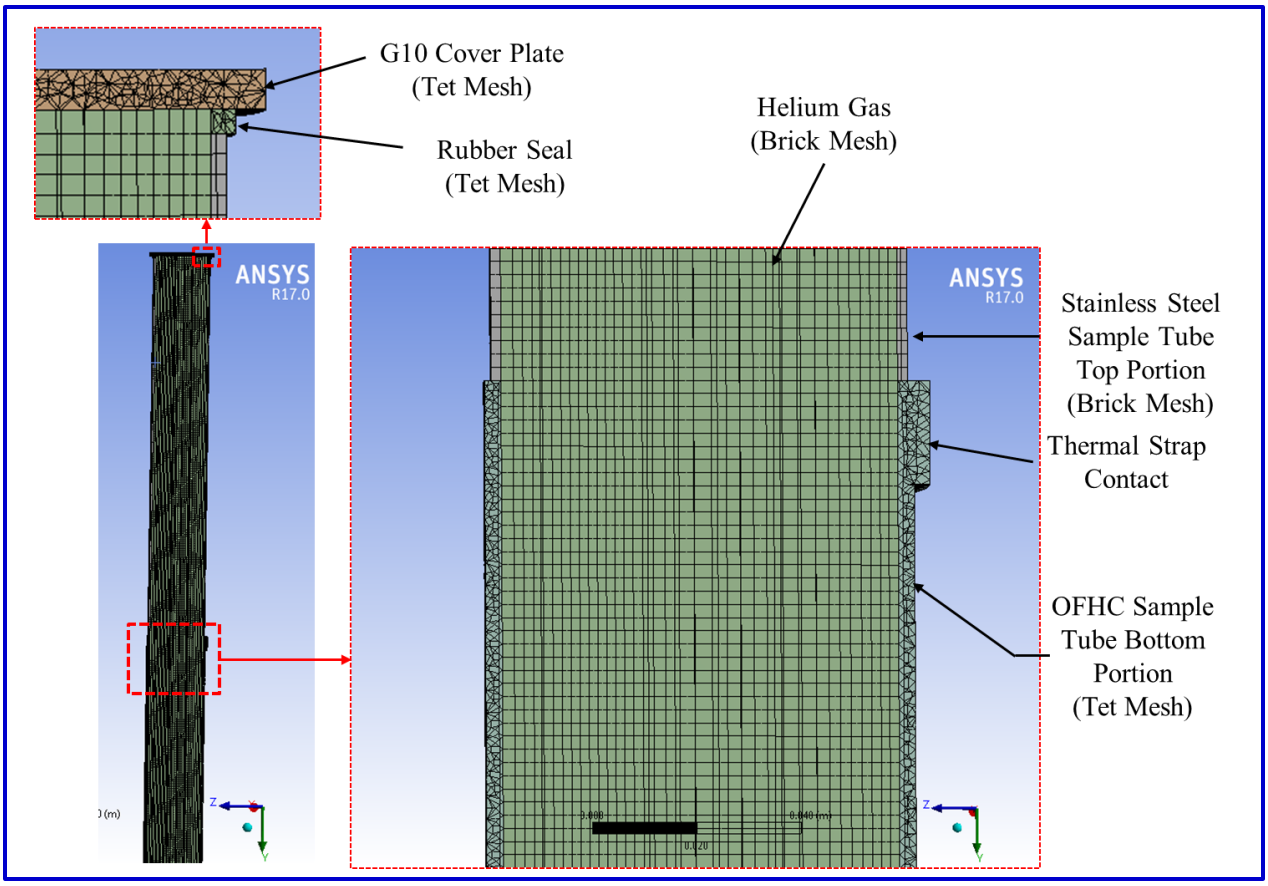

Figure 1313. Fluent model mesh

4.5 Results

The results of the solid model in thermal simulation steady state revealed that the sample tube remains close to a temperature of 4.2 K from the thermal strap all the way to the bottom (Figure 14). The different layers of insulation are also observed to provide the efficiency necessary to keep the temperature in the sample tube around a temperature of 4.2K. In term of verifying the accuracy of the results, we are relying on supplier provided temperature measurement of the sample tube at the thermal strap and in the bottom portion of the sample tube. A comparison with the simulation results shows that the model is effectively capturing the physics of the process.

.

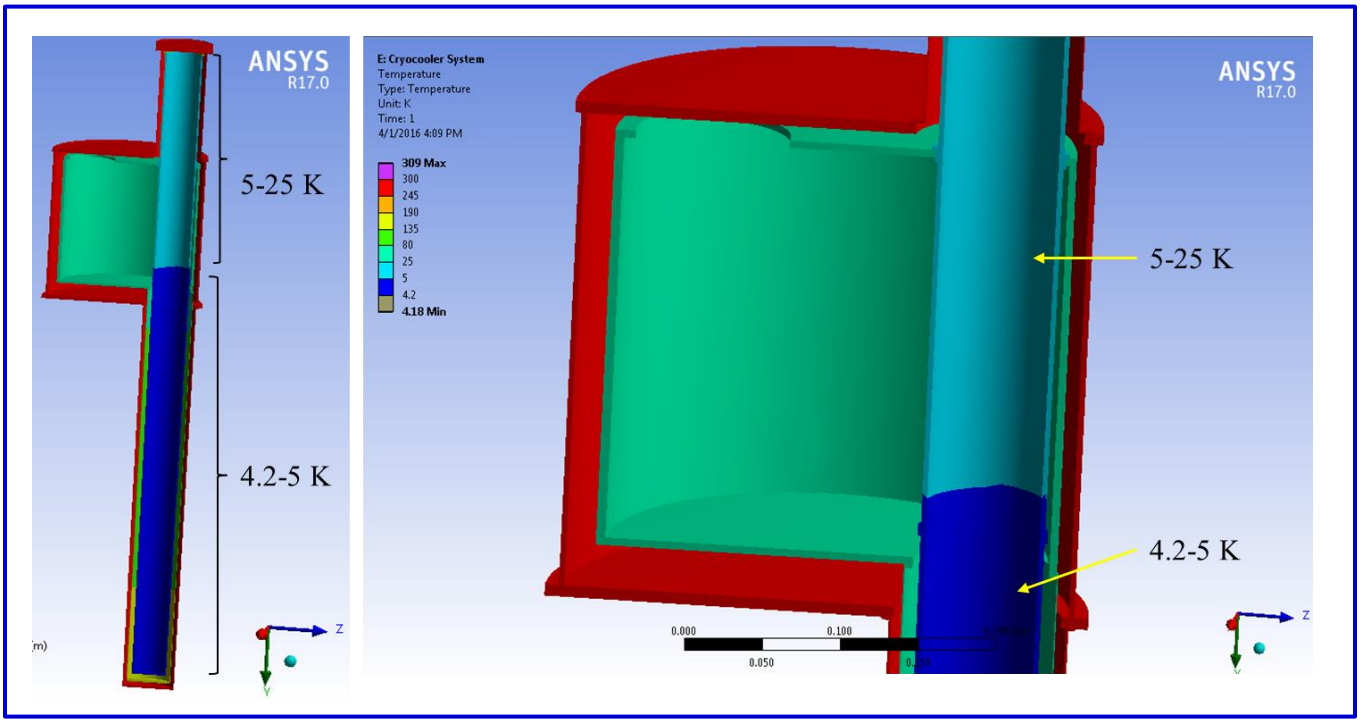

Figure 1414. Temperature profile of solid model

The Fluent model provided the temperature distribution throughout the helium gas and the sample tube (Figure 15). The temperature from the thermal strap down is around 4.2 K, as it was observed for the solid heat transfer model. There was no expectation that the results would be different as the heat source and heat sink have not changed. With these results, we are able to also say that the helium does take the temperature of the adjacent solid.

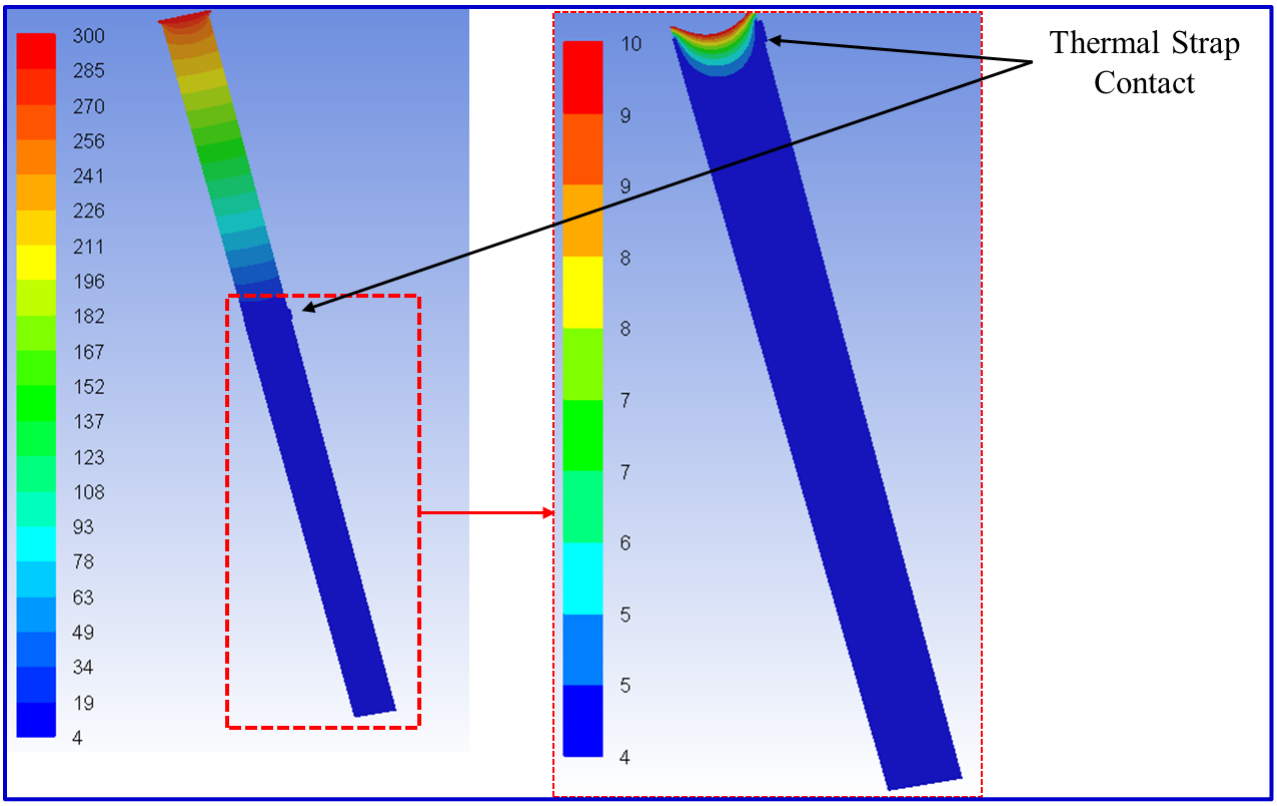

Figure 1515. Temperature (degree Kelvin) profile of fluent model

The radiation effect inside the sample tube did not seem to affect the temperature profile when compared to another case where the radiation affect was taken into account, the two are almost identical. Radiation is function of emissivity, but mainly temperature and view factor between the viewing surfaces. It requires a temperature difference between the viewing surfaces that is an order of magnitude high enough in order for radiation to become an important heat transfer method. For instance, considering the temperature difference between two surfaces one at 5 K and the other at 10 K with a view factor of 1 and emissivity of stainless steel at 0.07 can produce heat by radiation of 0.04 W. The other important element here is the view factor that is a function of the distance separating the radiating surfaces. The larger the distance is, the smaller the view

factor and vice-versa. Considering the top and the bottom of the sample tube, given the distant that separates them, the view factor is 0.0008. It is almost as if the top does not see the bottom.

The effect of conduction were then considered by modeling a G10 and a copper stick that extended from room temperature to the lower part of the sample tube. This model is the same as the previous model except for the added stick. The results are shown in figure 15. In this simplified model, heat from the room temperature is allowed to make its way to the bottom of the sample tube through conduction which is typically what takes places when the test rig hardware is in place. The effect of convection is also taken into account here.

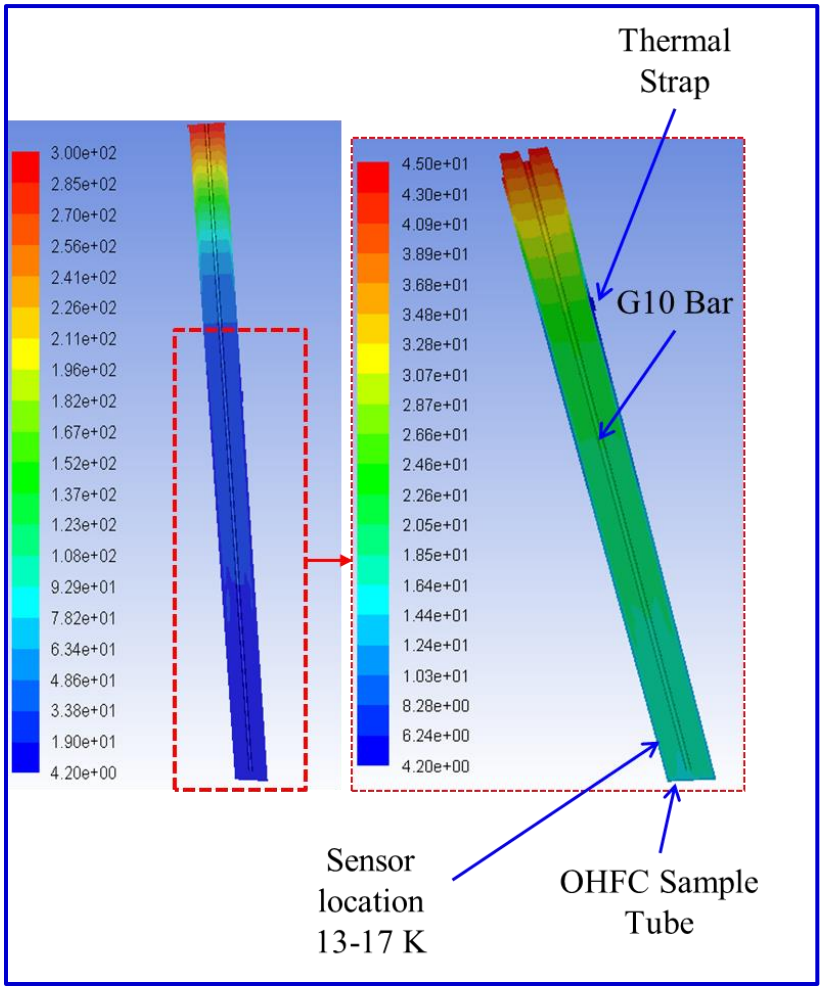

Figure 1616. Temperature distribution with inserted G10 Rod

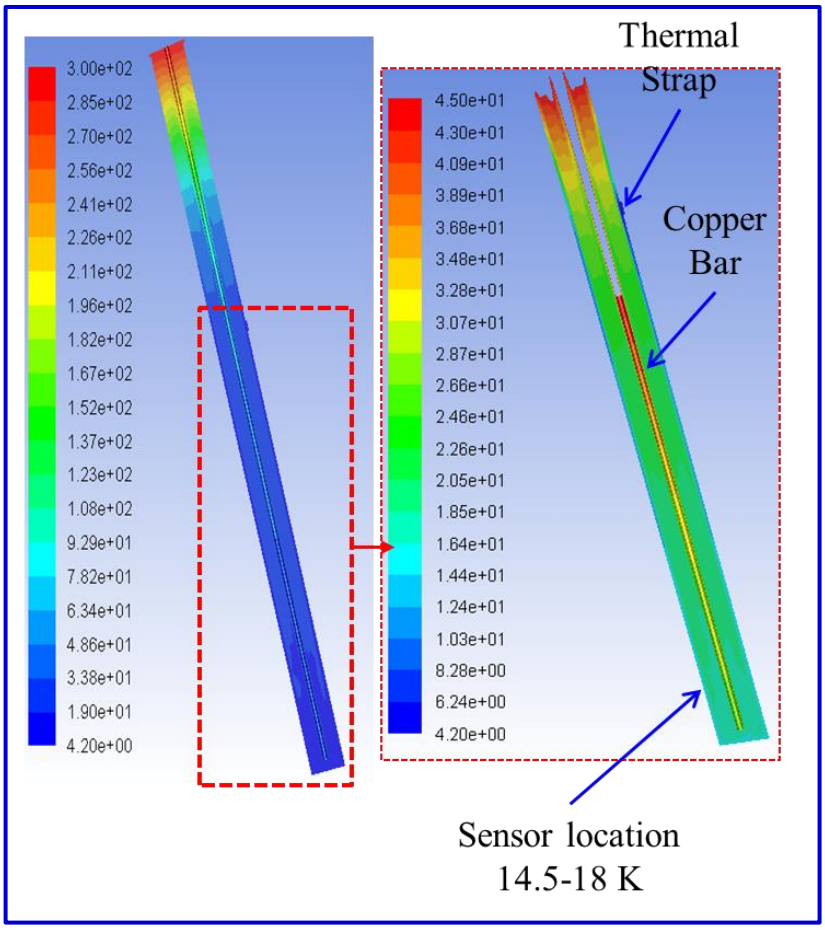

Figure 1717. Temperature distribution with inserted OFHC copper rod

In the sample area, the temperature distribution with the inserted copper rod setup is slight higher than the setup that uses a G10 fiberglass rod. The results suggest that using a test rig made out of G10 reduces the heat load inside the sample tube therefore allows for lower temperature to prevail. In the event that the superconducting sample is tested for current carrying capability, the results indicate that a test rig made out of G10 fiber glass would be more efficient. On the other hand if the sample is to be loaded in tension to a point where G10 does not have the required buckling strength and something stronger such as stainless steel is to be used to support the test rig, then we should expect higher heat loads inside the sample tube and therefore higher temperatures around the sample. The results of the copper case indicate that the higher the

conductivity of the material that is being inserted in the cryostat, the higher the temperature that will be reached in the sample area. The same will be true if the rod inserted is made out of stainless steel. It is a tradeoff between keeping low temperatures with a low strength test rig versus having one that produces a significant amount of heat but has a good strength.

Chapter V: Radiation Shields

The radiation was shown to be somewhat of a contributing factor to heat rise inside the sample tube in the previous section even though very low, so in this chapter we try to look more into ways to mitigate the effect it might have on keeping the temperature at 4.2 K in the sample area by addition of radiation shields. The effect of radiation becomes significant to heat rise at the bottom of the sample tube, when there is a conductive path between the exterior and the internal control volume by the mean of hardware protruding to the outside and therefore driving the heat into that sample tube. This chapter focuses on determining the adequate number of radiation shield and the most adequate location that would yield the most efficiency in keeping the lowest temperature possible at the bottom of the sample tube. As mentioned previously, radiative heat transfer requires a great temperature difference between the hot and cold surfaces element to have a significant impact. This radiation heat transfer study only takes into account the conduction effect; the fluid is removed from the model to simplify the analytical approach. There are essentially three models that are simulated in this section:

- A model with one dimensional radiation heat transfer to determine the number of shields required to results in the least heat generated by radiation at the bottom of the sample tube.
- A model with one dimensional heat transfer to highlight the effect of the emissivity on reducing the heat transfer by radiation.
- The last model is a multi-dimensional radiation heat transfer model with five radiation shields in two configurations, one where the shields are one centimeter apart and the second one where they are ten centimeters apart.

5.1 Assumptions

- Steady state heat transfer condition inside the cooling chamber
- For simplified hand calculation, all surfaces involved in the radiation process are gray and diffuse surfaces. Radiation is a function of emissivity which varies as a function of surface temperature wavelength and direction of the emitted radiation. The emissivity of a surface represent it ability to emit radiation in comparison to a blackbody at the same temperature. A blackbody emitted radiation is independent of direction and no surface can emit more energy than a blackbody. To simplify the phenomenon, a diffuse and gray surface can be used. A gray surface is characterized by having properties that are independent of wavelength. A diffuse surface has properties that independent of direction.
- The boundaries formed between two shields and surrounding cylinder is considered to be one enclosure that does not interact with the adjacent enclosures Figure 18.

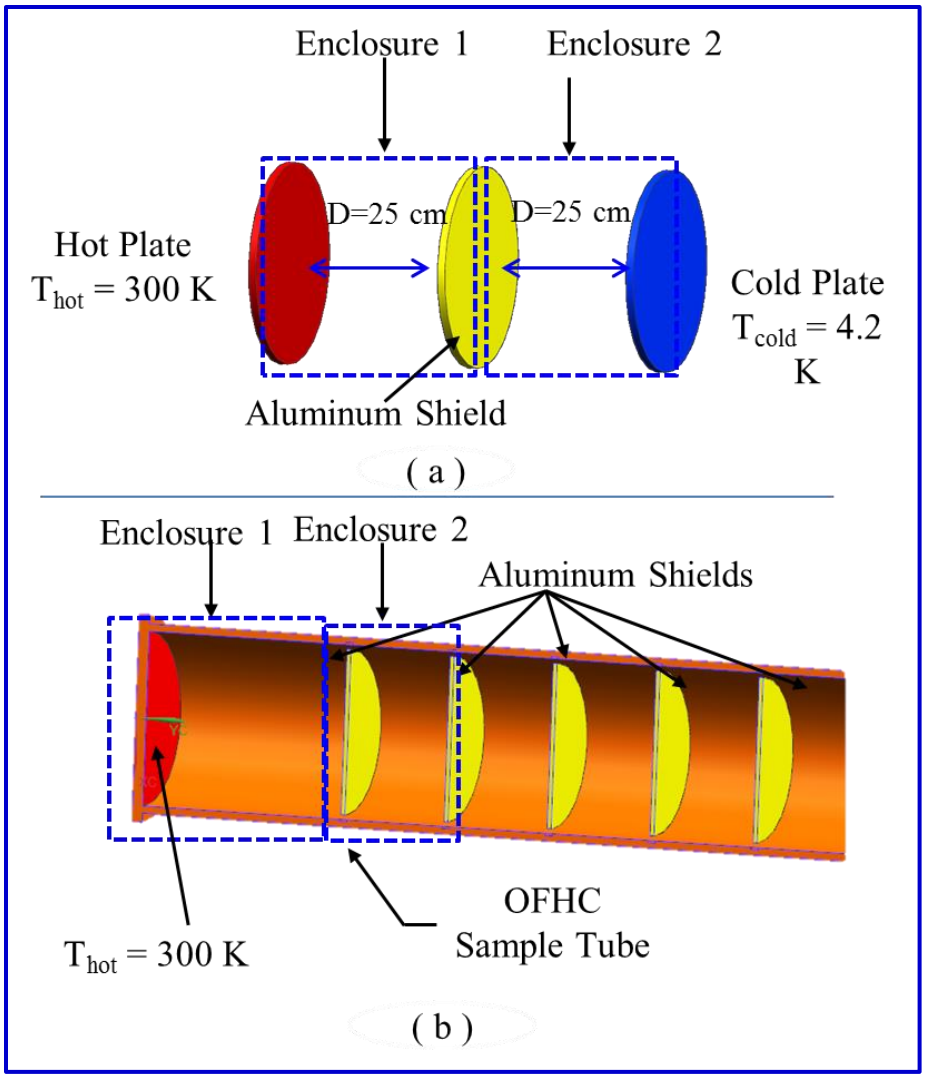

Figure 1818. Radiation models, a) Disk model for surface to surface one direction radiation study. b) Model for radiation study with vertical and lateral boundaries

5.2 Analysis

The first part of the radiation study uses a simplified model to that only looks at radiation in the vertical direction to determine how many and where the shield would produce the most benefit. In this case the radiation between the shields and the lateral wall of the sample tube are taken into account. The main assumption is that the only source of heat that could cause radiation is

originating from the top cover of the sample tube. The simplification allows backing-up the FEA analysis with a simple hand calculation as shown the subsequent section.

5.2.1 Radiation Heat Transfer without a Shield

The rate of radiation heat transfer between two disks spaced by distance L and having respective radius r_1 and r_2 is given by:

$$q_{1-2} = q_1 = q_2 = \left(\frac{T_1^4 - T_2^4}{\frac{1-\varepsilon_1}{\varepsilon_1} + (1/(F_{1-2}) + \left(\frac{1-\varepsilon_2}{\varepsilon_2}\right)} \right) * \sigma \qquad (5)$$

Where:

- T_1 is the temperature of the heat source 300 K
- T_2 is the temperature of the heat sink 4.2 K
- ε_1 and ε_2 are the respective emissivity of the heat source and the heat sink surfaces. This is function of surface finish.
- $F_{1\text{-}2}$ is the view factor calculated using the following equation:

$$F_{1-2} = \frac{1}{2} * [S - \sqrt{S^2 - 4 * \left(\frac{r_2}{r_1}\right)^2}] \qquad (6)$$

Where:

$$S = 1 + \frac{1 + \left(\frac{r_2}{L}\right)^2}{\left(\frac{r_1}{L}\right)^2} \qquad (7)$$

It is important to note that the view factor is inversely proportional to the distance separating the viewing surfaces and that the further apart the surfaces are the smallest the view factor, the smallest the heat transfer by radiation.

5.2.2 Radiation Heat Transfer with One Shield

By introducing one radiation shield the heat transfer equation above can be rearrange to add the resistant term of the shield. That is the equation becomes:

$$q_{1-2} = q_1 = q_2 = \left(\frac{T_1^4 - T_2^4}{R_1 + R_2}\right) * \sigma \qquad (8)$$

Where:

$$R_1 = \left(\frac{1-\varepsilon_1}{\varepsilon_1}\right) + (1/(F_{1-s}) + \left(\frac{1-\varepsilon_s}{\varepsilon_s}\right) \qquad (9)$$

And:

$$R_2 = \left(\frac{1-\varepsilon_s}{\varepsilon_s}\right) + (1/(F_{s-2}) + \left(\frac{1-\varepsilon_2}{\varepsilon_s}\right) \qquad (10)$$

By reviewing this equation closely it does point out to the fact that the addition of a shield increase the total resistance term which in return decrease the heat flux between the two surfaces.

The temperature for each of the shields can be determined using the Kirchhoff law of current applied to heat transfer. The temperature at the shield can be written using the following equation [16]:

$$T_s = [T_1^4 - \left(\frac{R_1}{R_{tot}}\right) * (T_1^4 - T_2^4)]^{0.25} \qquad (11)$$

5.2.3 Radiation Heat Transfer with Three or More Shields

With the additions of shields, the heat rate equation remains the same however there is an increase in the number of resistance preventing the heat from travelling from the heat side to the cold side.

$$q_{1-2} = q_1 = q_2 = \left(\frac{T_1^4 - T_2^4}{R}\right) * \sigma \qquad (12)$$

Where:

$$R = R_1 + R_2 + R_3 \ldots \qquad (13)$$

Each resistant above has a similar expression to R_1 previously shown. In the expression of the resistance, it is important to see that in order to improve the efficiency of a shield, the top and bottom can be given different surface polish, with the finer polished side of the shield facing the hottest enclosure. The emissivity and temperature difference are the factors that drive radiation; the hot surface facing a very finely polished surface can become a great baffle. And inversely the opposite side facing the cold section shall be made to have high emissivity, so that less heat is driven to the bottom of the sample tube.

5.3 Results

The first part of the exercise was to show that the introduction of the radiation shield does prevent a temperature increase down below at the heat sink using a one dimensional heat transfer approximation.

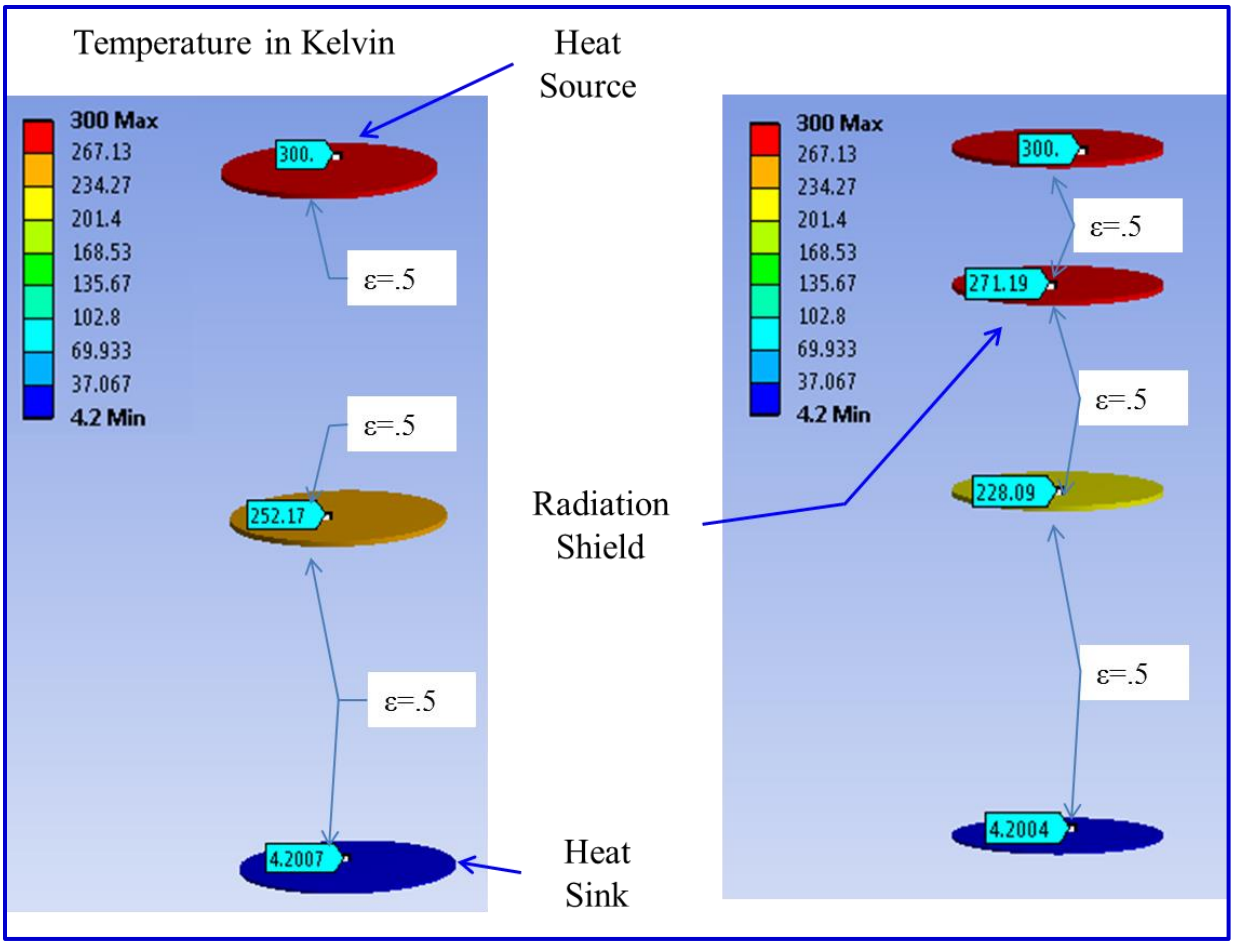

Figure 1919. One Radiation Shield in One Directional Heat Transfer

The temperature of the mid plate goes from 257 K to 228 K with the addition of one radiation shield (Figure 19).

It is then verified that the addition of shields does drive the temperature of the mid plate down as the number of shield is increased (Figure 20). This confirms what was laid out by equation 12, where the more shields are added, the less the heat transfer rate becomes.

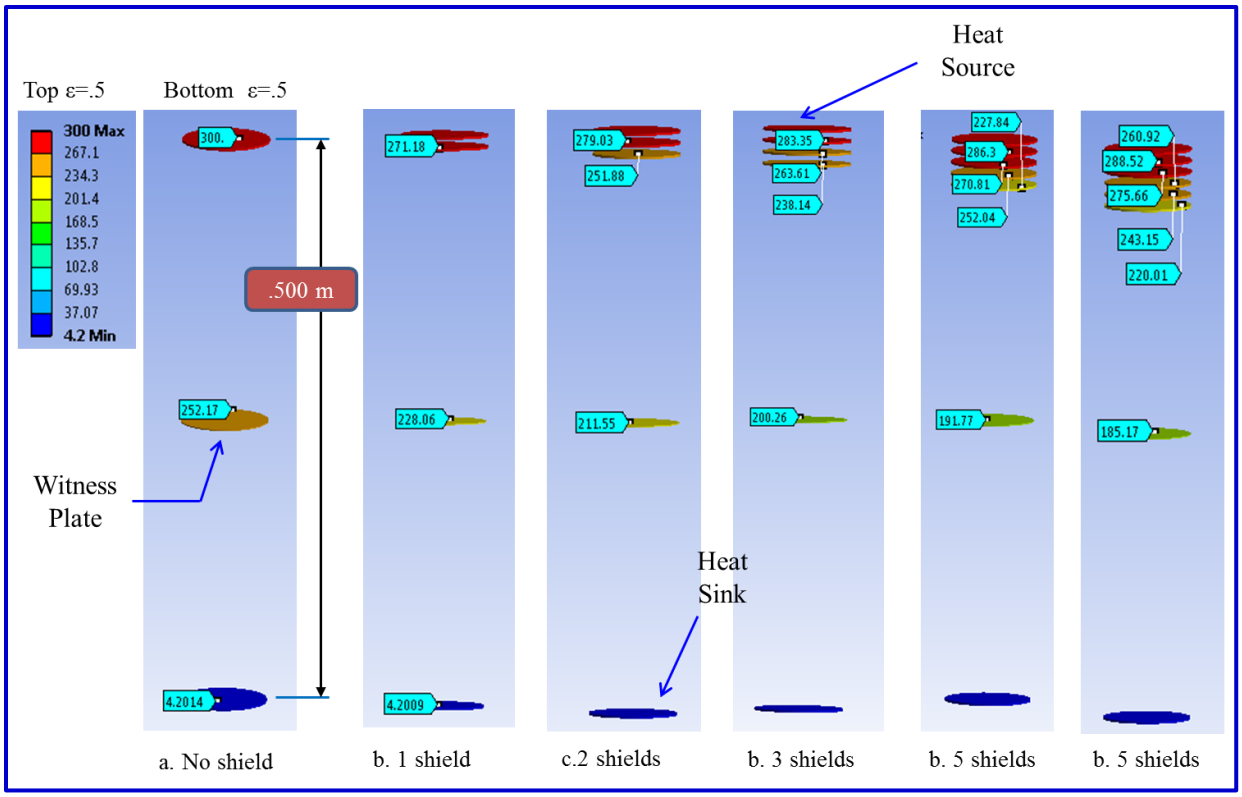

Figure 20. Radiation shield effect in one directional heat transfer

With these results the graph below was developed to provide a visual insight of the adequate number of shields that can be utilized before the addition of shields cannot be justified, see figure 21.

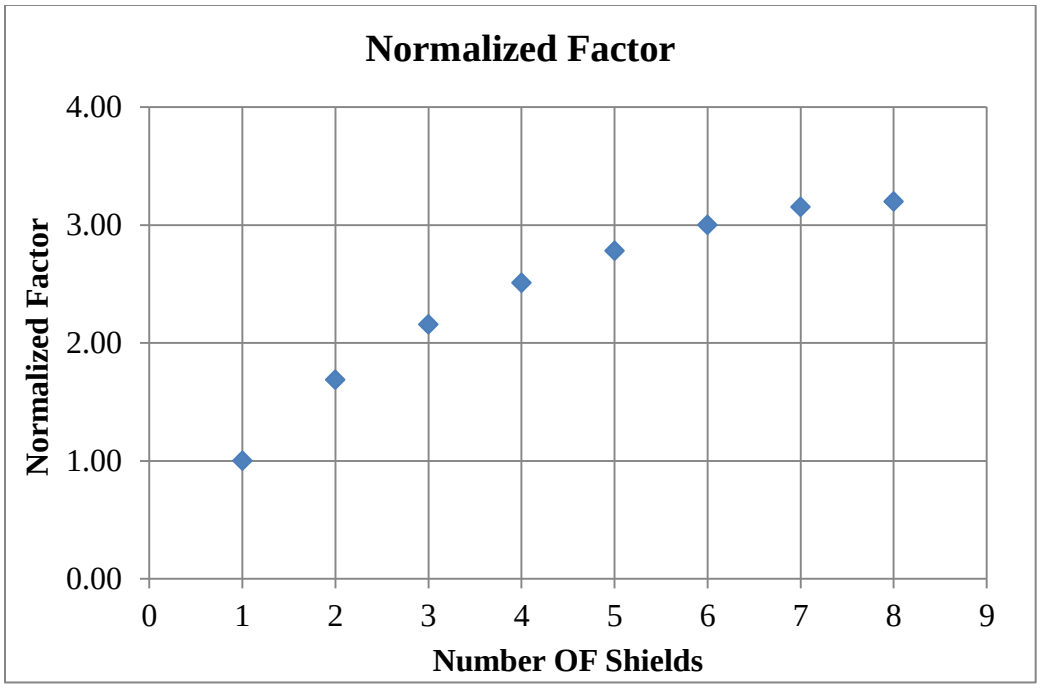

Figure 2121. Normalized temperature reduction factor Vs number of shields

The plot above indicates that the addition of one shield provides a good blockage to heat transfer by radiation but the addition of shields does not make it much greater beyond three shields. Also the study showed that the location of the shield did not make much difference.

The next aspect of the radiation is considered in the analysis for the one dimensional heat transfer is the effect of the emissity on the radiation shield. An emissivity of 0.5 is considered for all the surfaces that are participating in the radiation process in figure 19 a. The emissivity in next setup is made such that the top of the shield is well polished so it has an emissivity of 0.05, while the other surfaces have an emissivity of 0.5.Temperature of the shield midway shows a noticeable difference in temperature as the emissivity on the top side of the shield is decreased (Figure 22). This shows how the use of fine polished shield can be beneficial in intercepting radiation. Table 1 shows the emissivity of technical material at a wave length of about 10 μm at room temperature. Note that stainless steel is commonly available with an emissity of 0.07,

which could the reason for finding this material serving as the outer layer insulation for the cryocooler.

Table 1. Emissivity of technical materials at wavelength of about 10 μm at room temperature [18]

Material	Emissivity		
	Polished	Highly Oxidized	Common Condition
Copper	0.02	0.6	-
Aluminum	0.03	0.3	-
Brass	0.03	0.6	-
Stainless Steel	-	-	0.07
Glass	-	-	0.9

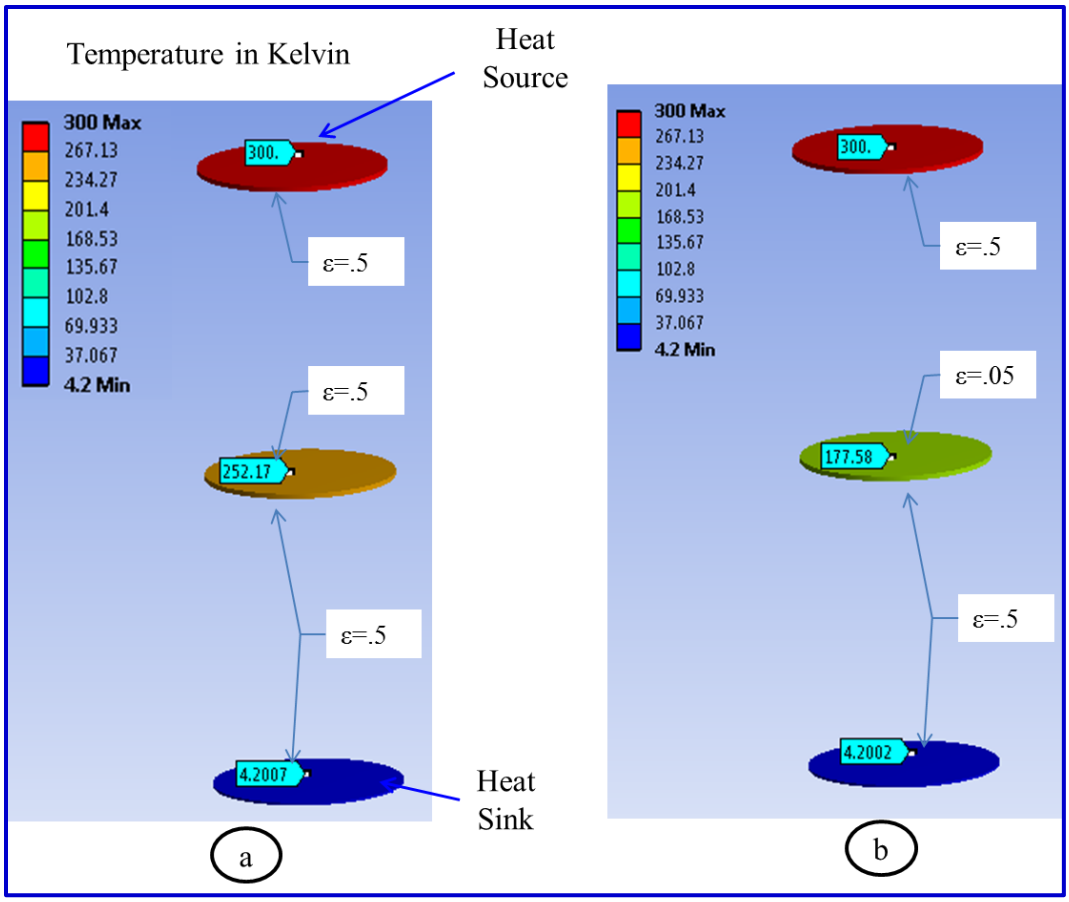

Figure 2222. a) Radiation with 0.5 emissivity on shield side facing heat source, b) Radiation with 0.05 emissivity on shield side facing heat source

In the last part of the radiation heat transfer study, the sample tube is considered with a setup of five radiation shields. In order to determine if there is a preferred positions where the shields can be placed that would be the most effective different spacing's are considered. In this case the heat transfer is not one dimensional, but is allowed to flow in all three dimensions. Two configurations are used to determine if the position of the shields would mater much to the outcome: one where the shields are closely stacked to each other (1 cm) toward the top of the sample tube and another where the shields are equally spaced (10 cm) apart.

The boundary condition is setup so that the temperature at the top of the sample tube is 300 K and the thermal strap interface is at 4.2 K. Radiation heat transfer for each enclosure is defined with emissivity of 0.5 for all the contributing surfaces (Figure 17.b). Conduction and radiations are the methods of heat transfer.

The results did not show much difference between the two configurations (Figure 22), one with shield stacked close to each other (1 cm) and the other where the shields are further apart (5 cm), therefore the radiation shields can be placed anywhere in the sample tube with the expectation that the same results will be obtained. The radiation effect is very negligible in steady state as long as there is no conduction form the room environment driving heat into the lower portion of the sample tube where the cold helium gas resides. The conduction is the dominant effect. As the test rig is in place in the cryocooler there could be significant conduction taking place and creating a temperature gradient that could potentially become a factor for heat by radiation to take place. In the meanwhile, the G10 plates that support the test rig can play a role in shielding the radiation heat that is trying to make its way to the bottom of the sample tube.

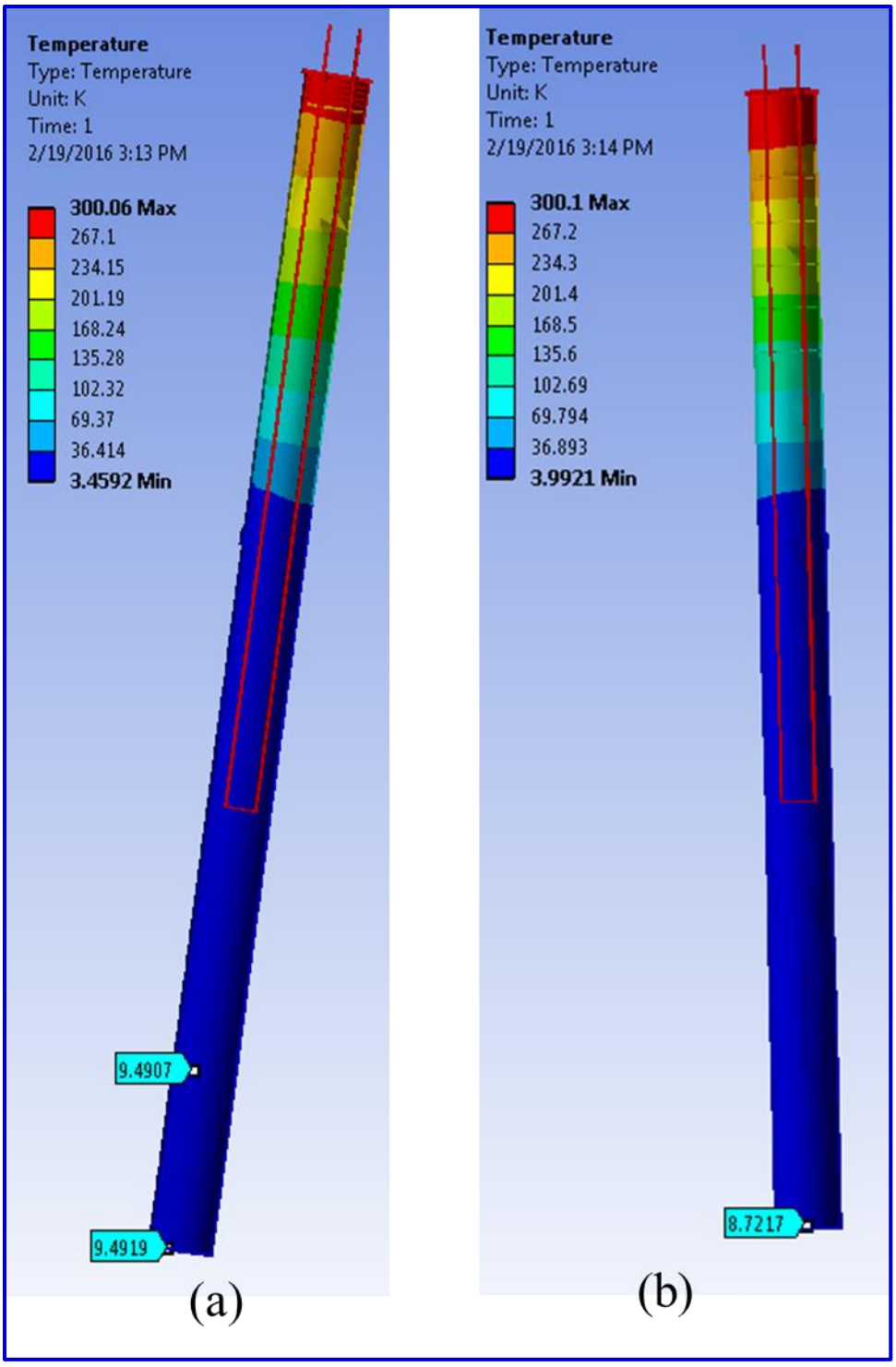

Figure 2323. Temperature distribution in the sample tube. (a) shields stacked 1 cm apart, (b) shields stacked 5 cm apart

Chapter VI: Summary and Future Work

6.1 Summary

Superconductor testing at low temperature is crucial in advancing some of the application where they can be beneficial in reducing energy consumption, creating more versatile medical equipment and much more life changing technologies. The Special SHI-950T-15 cryocooler allows testing superconducting samples at cryogenic temperature close to 4.2 K, where the sample is surrounded by a gas and not submerged in a liquid. This reduces the risk associated with operator contact with the cryogenic liquid, therefore, reducing some of the risks involved with working with such material at low temperature. It also offers an advantage by limiting the amount of fluid lost to boiling as it is the case when the sample is dipped in a liquid dewar. The superconductivity of a material is a function of temperature, current density and magnetic field; however, temperature is the most critical element that has to be provided to the material to attain superconductive properties. The other two represent an upper limit beyond which the material no longer behaves as a superconductor. It is therefore important in this thesis to perform a study of the environment surrounding the superconducting sample during the test, to insure the temperature remains low enough.

This study demonstrates that conduction is the main heat transfer method to keep the sample tube and its content cold inside the cryocooler. Heat transfer by convection method has very limited effect on keeping the temperature low in an empty sample tube, as the two required ingredient are not present, density gradient and body force. On the other hand, heat transfer by convection will become important when an element such as the test rig is allowed to drive heat to the lower portion of the sample tube. The radiation effects in steady state are found to be negligible

because of the low temperature difference between viewing surfaces and the distance that separates the heat source to the volume that needs to remain below 4.2 K.

The selection of the material for constructing the test rig is therefore crucial, as material with low specific heat would drive less heat into the sample zone. This might point to the benefit of using material with low thermal conductivity and low specific heat. The low thermal conductivity will limit the amount of heat that flows into the sample tube. Low specific heat material will allow less energy to cool down than one with high specific heat even though a high specific heat element would be beneficial in because it has more thermal stability. A material such as fiberglass G10 can be used to support the test rig and at the same time limit the heat conduction into the sample tube. The test rig design should take into account the material strength if the test is looking to test the tension capability of the sample and a trade study shall be performed to determine the most suitable material for such test.

6.2 Future Work

Superconductor testing expands beyond testing for current carrying capability, the strength of the superconductor wires is also important for various applications that researches are conducted in. The cryocooler that we have in the lab even though it operates in a controlled environment where the sample is placed in the helium gas and sealed to the exterior, it remains possible to mechanically drive the rig in putting the sample in tension for testing the capability of the HTS tape at a given temperature. There are two approaches that are described in reference 17.
The first approach is to convey a mechanical motion down the cryostat from room temperature to the inside of the cryostat by the means of rotating shafts, pull and push rods cord drive etc. The issue here is that, there is a high risk of introducing ice and or air into the system which might

results into a harmful situation. It is a good option though as far as being able to debug the code and to keep good control of the motion that is being imparted to the test sample.

The second approach drives the motion electrically at low temperature with motor widget inside the sample tube. This option might be feasible if it was not for the concern that very limited space is available inside the sample chamber which is 7.6 cm in diameter. The second option can be viable if the motor portion is taken out of the picture and alternate mean for producing motion are considered.

The rig can be constructed to rely on thermal expansion to create the motion that is required to put the sample in tension. The motion will be very limited and will require the initial sample set-up to be very precise. The other factor is that the thermal expansion will require the introduction of heat into the sample tube in which we are already trying to keep cold in the first.

Thermocouple can be used to monitor the temperature and strain gages to quantify the deflection amount.

The final idea would be to construct a test rig that would allow for motion of the test specimen using an external magnetic field (Figure 24).

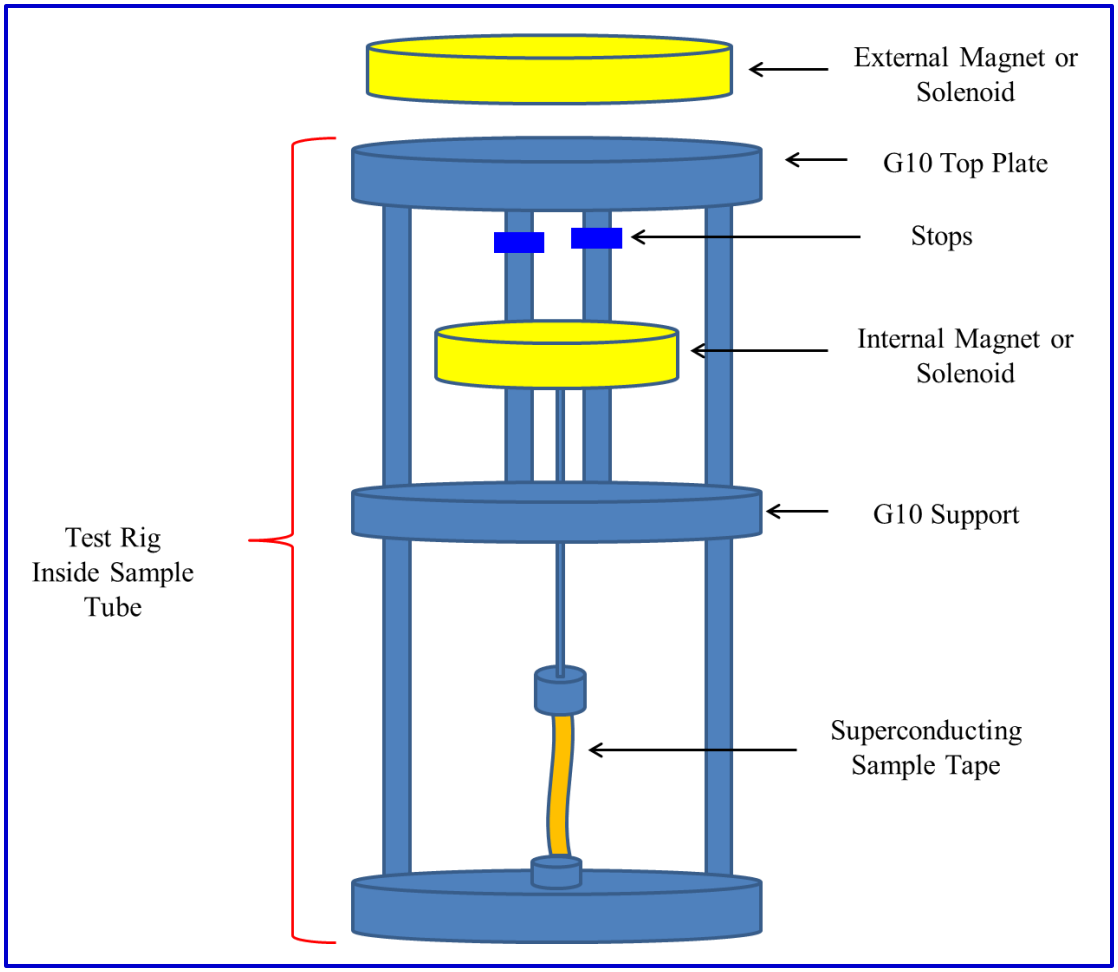

Figure 24. Test rig for tension testing of superconductor wires

A study shall be conducted to determine the interaction such a set-up might have with magnetic susceptible parts that are present on the cryocooler and inside the sample tube. The advantage of this method is that there is no external drive that has to make its way inside the cryostat, therefore eliminating the risk of ice formation in the system.

Appendix I: Photos of Cryostat, Compressor and Water Chiller & Specs

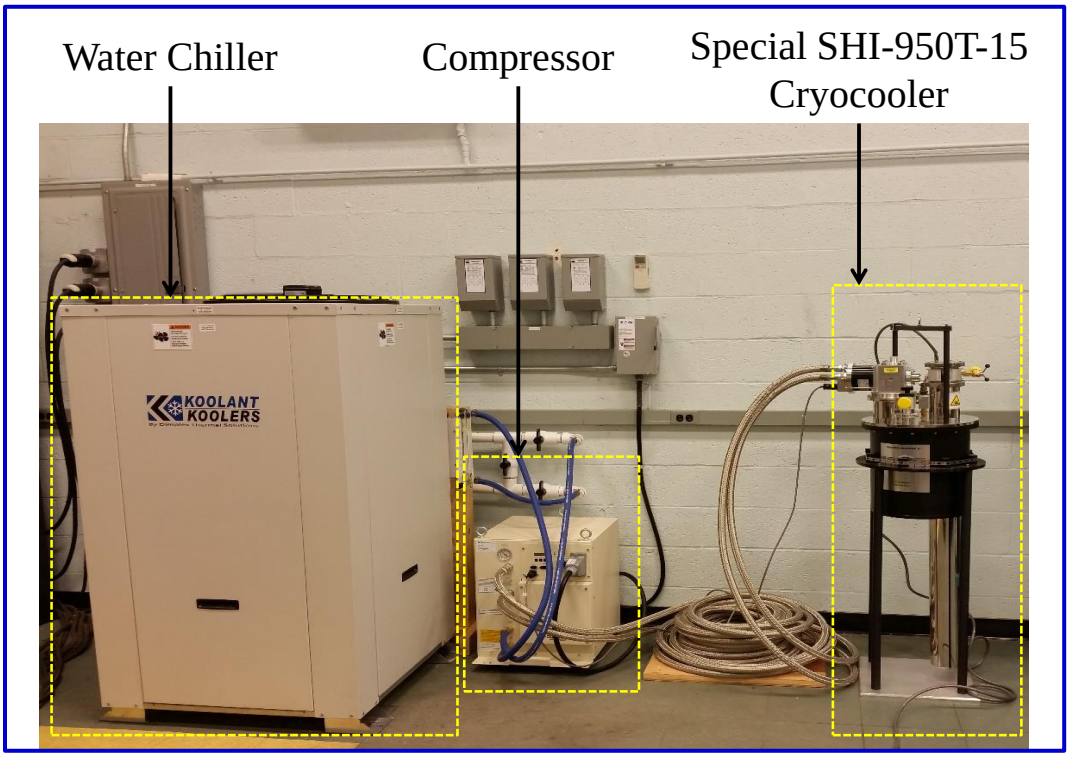

Figure 25. Equipment Overview

Figure 26: Cold head RDK-415D [7]

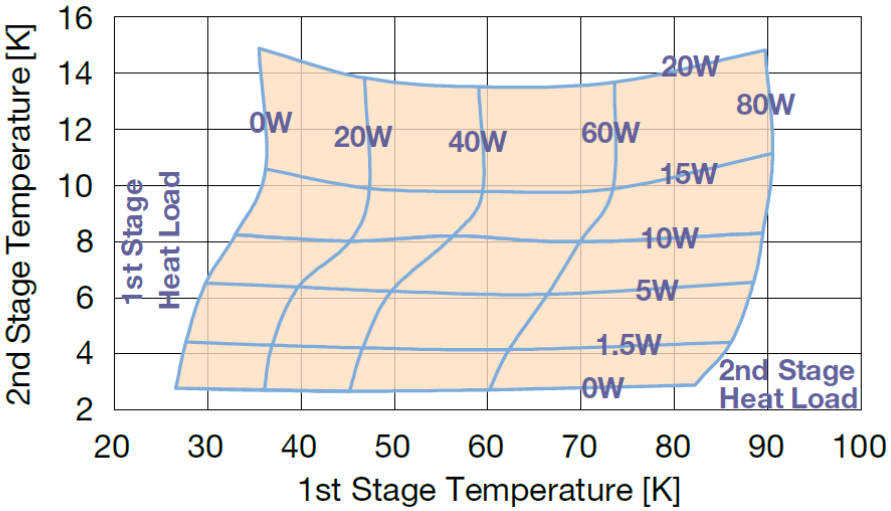

Figure 27: RDK-415D cold head capacity map (60 Hz) [7]

Table 2. Cold head specification RDK-415D [7]

Power Supply Hz	**50**	**60**
2nd Stage Capacity Watts @ 4.2 K	1.5	1.5
1st Stage Capacity Watts @ 50 K	35	45
Cooldown Time to 4.2 K Minutes	60	60
Weight kg (lbs.)	18.5 (40.8)	
Maintenance Hours	10,000	

Table 3. Cryocooler temperature test validation [7]

JOB #	**17641**		**SENSORS**					
TEST DATE	**8/6/14**		**CH A**	**CH B**	**CH C**	**CH D**		
LAB TECH	**JMC**	**MODEL**	**DT-670B-SD**	**DT-670B-CU**	**DT-670B-CU**			
CRYOSTAT MODEL	**SHI-950**	**LOCATION**	**SAMPLE TUBE**	**SAMPLE POSTION**	**SECON STAGE**			
SALES PERSON	**BK**	**S/N**	**D6036786**	**LAB**	**D6043144**			
COMPUTER	**YiZ-W7**							

COMMENTS																					
Heater range / Max current chart																					
Heater range:			**Max current:**									**MODEL / S/N**									
#0 : Off			**#0 : User**					**COLDHEAD**				**RDK-415D2/AHD14022**									
#1 : Low			**#1 : 0.707A**					**COMPRESSOR**				**F70L/FN00907**									
#2 : Medium			**#2 : 1A**					**COMPR. VOLT/FREQ**				**208/60Hz**									
#3 : High			**#3 : 1.414A**					**LHE LEVEL METER**													
			#4 : 2A					**TEMP. CONTROLLER**				**LAB**									
											Heater resistance (Ω)								**Heater resistance (Ω)**		
								Output 1			**50**				**Output 2**		**50**				
Elaps. Time	**Ch A**		**Ch B**		**Ch C**		**Ch D**	**Set point**	**Heater range**	**Max Current**	**Heater output**	**P**	**I**		**Set point**	**Heater range**	**Max Current**	**Heater output**	**P**	**I**	
(Min)	**K**	**V**	**K**		**K**		**K**	**K**	**SEE CHART**		%				**K**	**SEE CHART**		%			
224.3	7.54	1.46			5.62	1.53	0	0	0	0	0	0	50	20	0	0	0	0	50	20	
571.7	5.11	1.55			4.17	1.58	0	0	0	0	4	0	50	20	0	0	0	0	50	20	

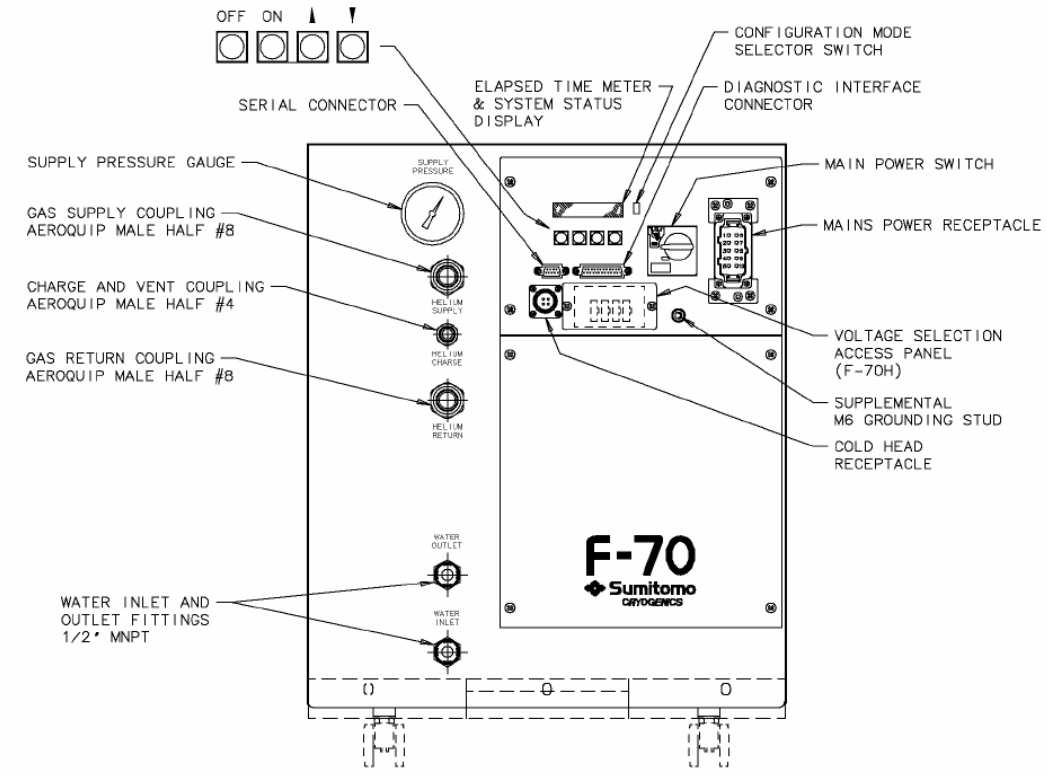

Figure 28: F-70H and F-70L compressors, front view [10]

Figure 29. Turbomolecular pump model TS75D1002 [9]

Appendix II: Material Properties

Superconductor Critical Temperature, LTS & HTS,

Table 4. Critical temperature (Tc), crystal structure of some low temperature superconductors [29]

Material	Tc (K)
Al	1.2
Hg	4.15
Mo	0.92
Nb	9.26
Pb	7.19
Sn	3.72
Ta	4.48
Ti	0.39
V	5.3
Zn	0.88
Nb_3Sn	18.05
Nb_3Ge	23.2

Table 5. Critical temperature (Tc), crystal structure of some high temperature superconductors [4]

Material	Tc (K)
$Bi_2Sr_2CuO_6$	20
$Tl_2Ba_2CuO_6$	80
$Bi_2Sr_2CaCu_2O_8$	85
$YBa_2Cu_3O_7$	92
$HgBa_2CuO_4$	94
$Tl_2Ba_2CaCu_2O_8$	108
$Bi_2Sr_2Ca_2Cu_3O_{10}$	110
$T_lBa_2Ca_3Cu_4O_{11}$	122
$Tl_2Ba_2Ca_2Cu_3O_{10}$	125
$HgBa_2CaCu_2O_6$	128
$HgBa_2Ca_2Cu_3O_8$	134

Thermal Conductivity

Table 6. Conduction coefficient for selected material [18]

Conduction Coefficient				
Temp K	Conductivity OFHC W/m-K (RRR=100)	Conductivity Polymer G10 W/m-K	Conductivity AL 6061-T6 W/m-K	Conductivity Stainless Steel W/m-K
4	630	0.072	5	0.27
10	1540	0.11	14	0.9
20	2430	0.16	28	2.2
40	1470	0.22	32	4.7
77	544	0.28	84	7.9
100	461	0.31	98	9.2
150	418	0.37	120	11
200	407	0.45	136	13
295	397	0.6	155	15

Specific Heat Capacity

Table 7. Specific heat capacity for selected materials [18]

Specific Heat J/ Kg-K				
Temp K	Cp OFHC J/Kg-K (RRR=100)	Cp Polymer G10 J/Kg-K	Cp AL 6061-T6 J/Kg-K	Cp Stainless Steel AISI 316 J/Kg-K
4	0.10	2.00	0.29	2.00
10	0.86	15	1.57	5.20
20	7.51	47	8.90	17
30	26.5	81	33	10
50	96.3	149	149	100
77	195.9	239	348	200
100	255.3	317	492	250
150	324.1	489	713	350
200	359.0	664	835	400
300	389.4	999	954	480

Electrical Resistivity of Selected Material [18]

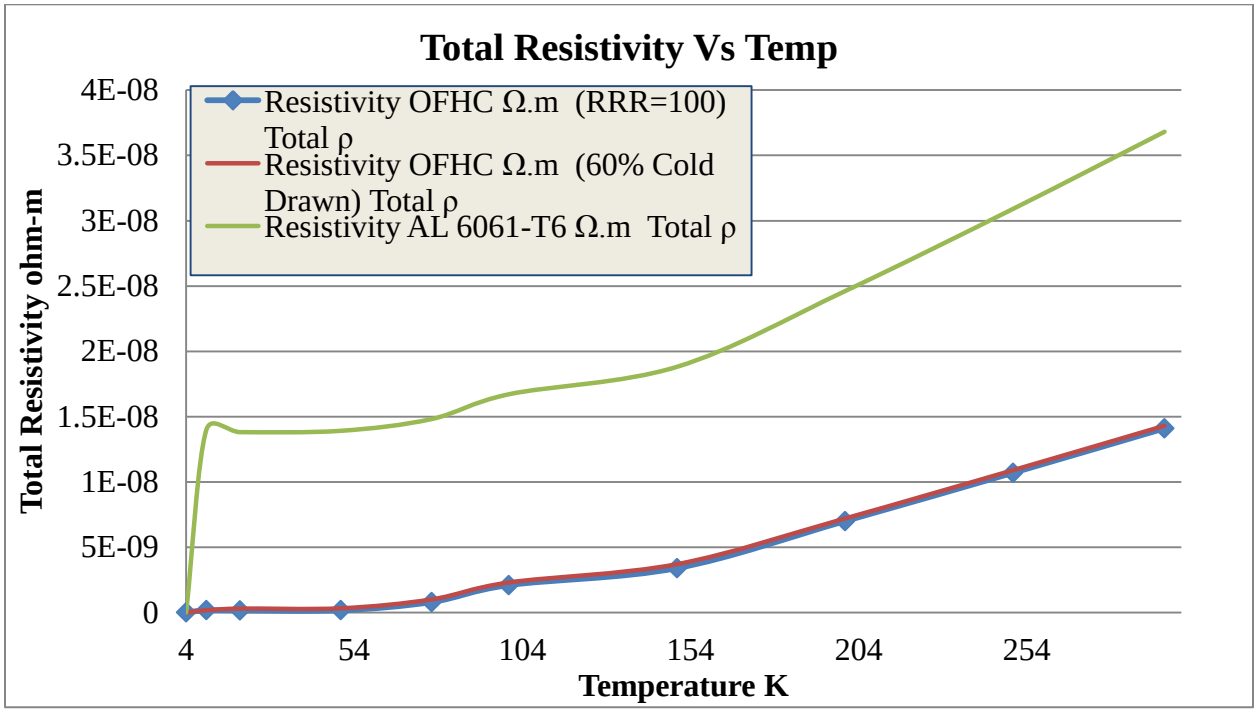

Figure 30. Total resistivity of selected materials [18]

Appendix III: Ansys® Files

Appendix 3.a: Fluent Model Set-up and Results

The model is built in Unigraphics® and then exported to ANSYS design modeler in a Parasolid format. In the example discussed in this section, the model consisted of the sample tube, the top cover and a copper stick that extends from the top cover to the lower portion of the sample tube as shown in figure 30 below. An important step in getting the model to work is to group all the parts into one even though they remain separated entities. Note that this approach will allow for a more uniform mesh at the shared boundaries between adjacent elements.

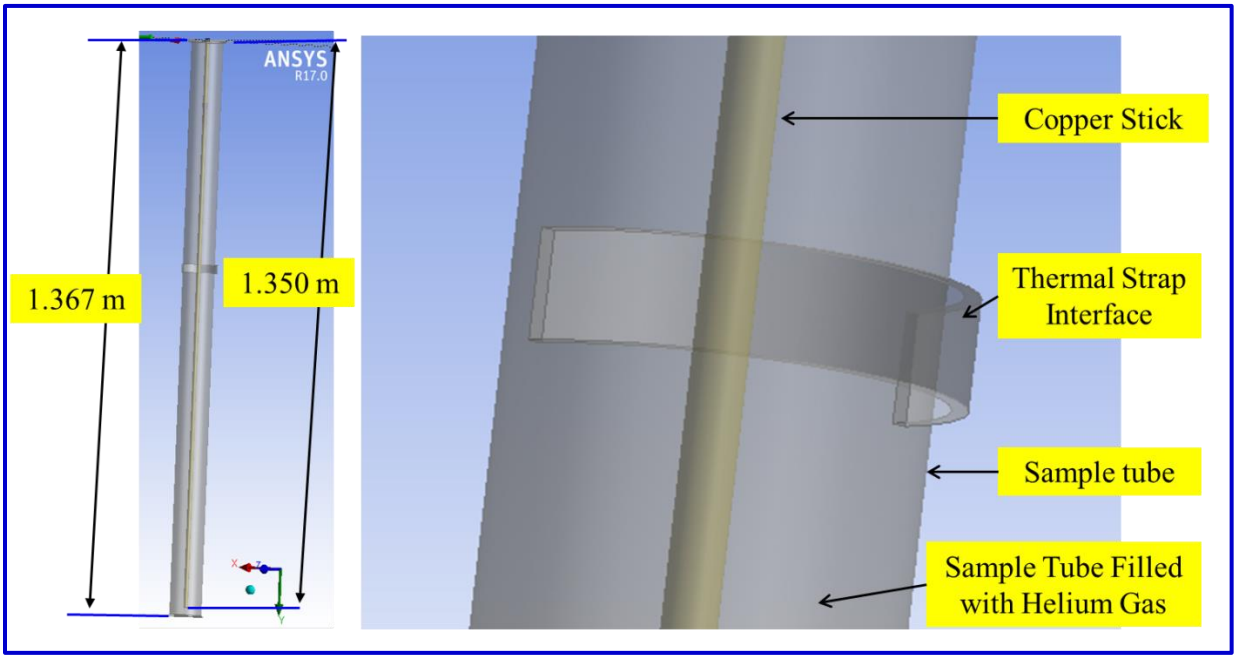

Figure 31. ANSYS Design Modeler view of Fluent® model

The model is then meshed in ANSYS Mechanical Design using mostly brick elements. The important part of this step is to create a named selection for each of the surfaces that the model has in order to place a boundary condition on them later in Fluent. A surface will be either insulated, coupled to the helium gas or will have a temperature boundary. The model is then

open in ANSYS Fluent after an updating the mechanical design mesh. At this point one should have a check mark in front of the geometry and Mesh within the simulation (Figure 31).

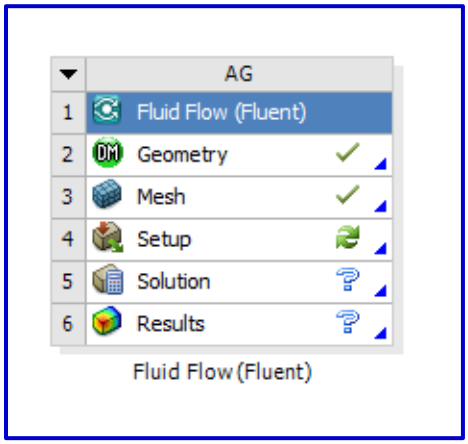

Figure 32. Fluent simulation when mesh has updated [21]

Fluent Setup

General

Enable the gravity option and the gravitational acceleration value in the Y direction to activate the free convection heat transfer method as shown in Figure 32 .

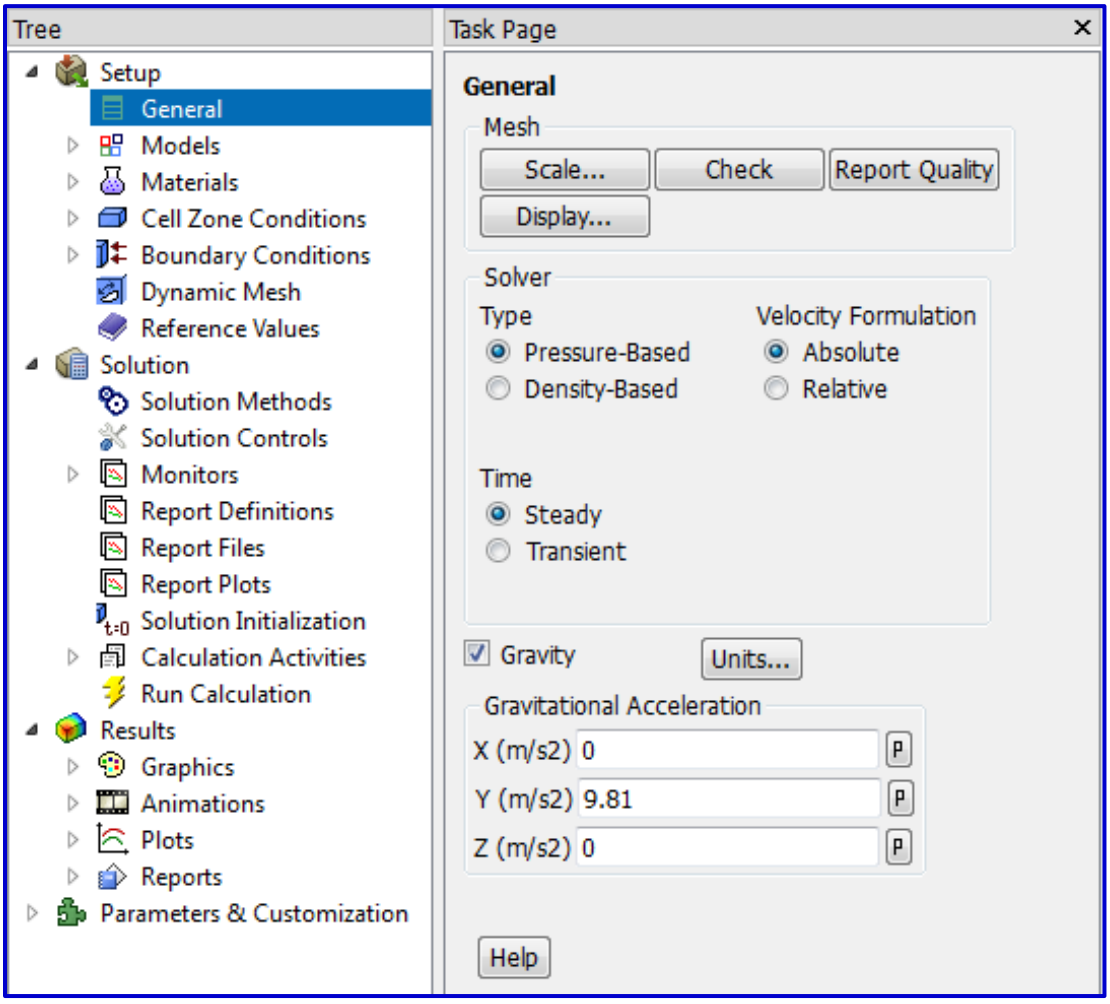

Figure 33. Fluent model - general setup [21]

Models

Enable the energy equation and setup the surface to surface radiation. The surface to surface radiation needs to be applied to all walls.

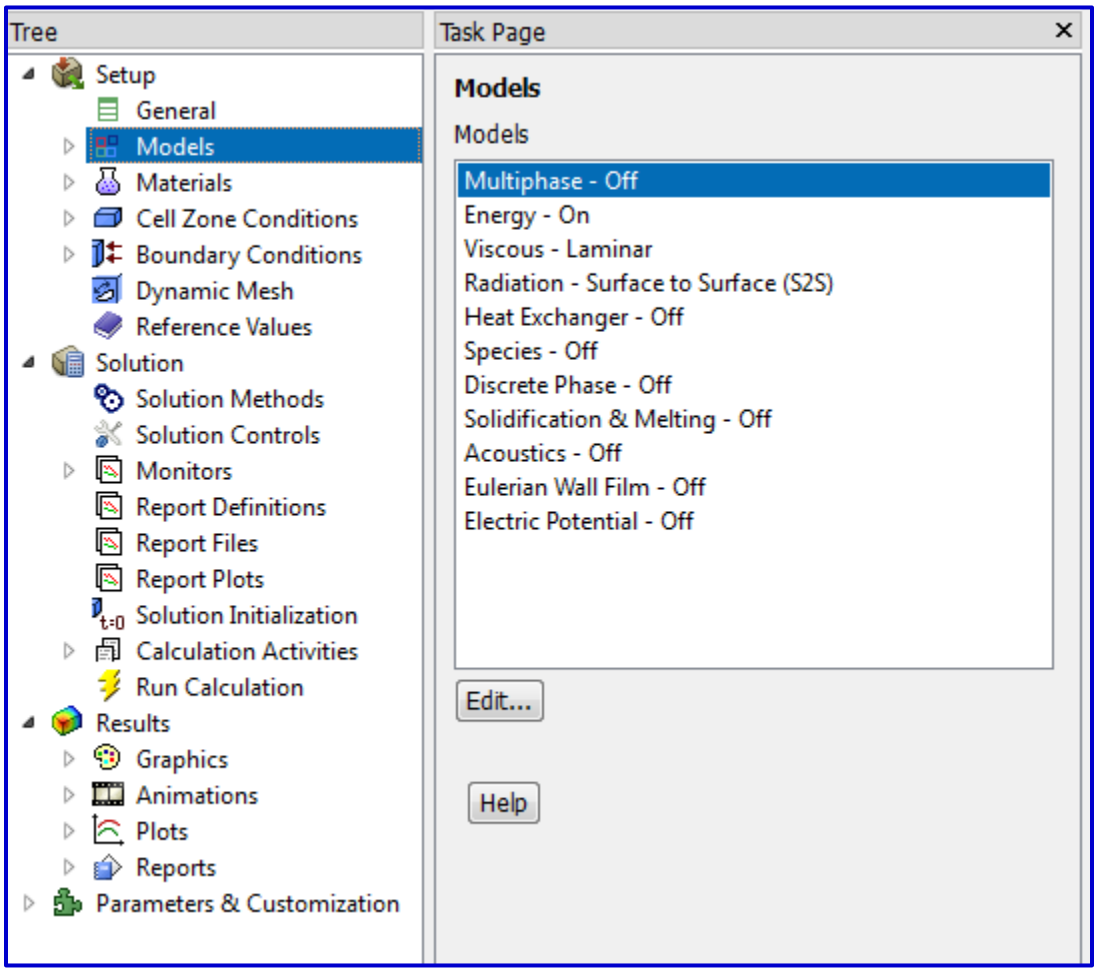

Figure 34. Model setup screen [21]

Materials

The material properties are setup using the piece linear tab under the constant properties of each material. Only the density of helium is setup to have ideal gas material properties. All the properties for the solids are found in reference 18. The properties for helium are taken at 1 atmosphere except for the density as stated above.

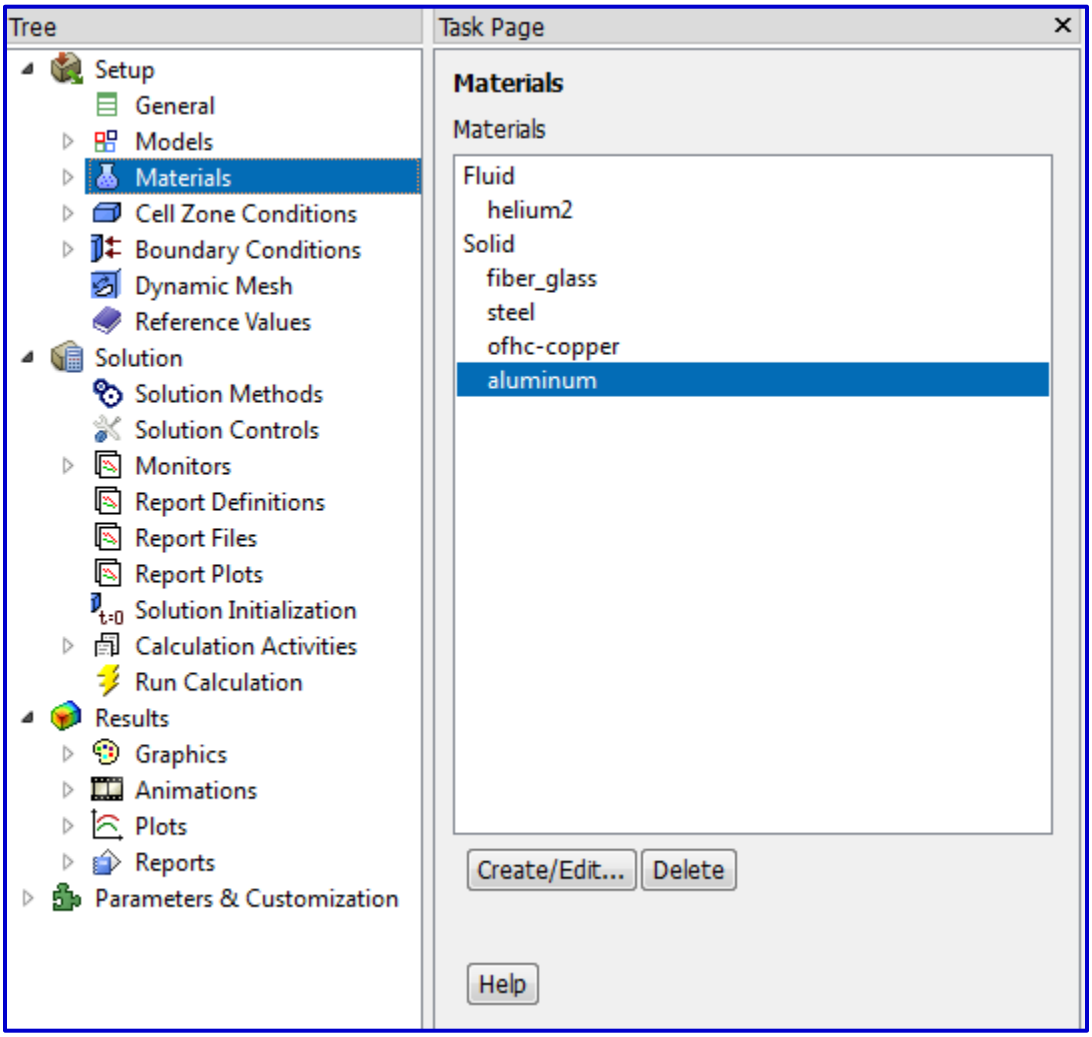

Figure 35. Material set up screen [21]

Cell Zone Conditions

This section assigns to each item of the model a material property.

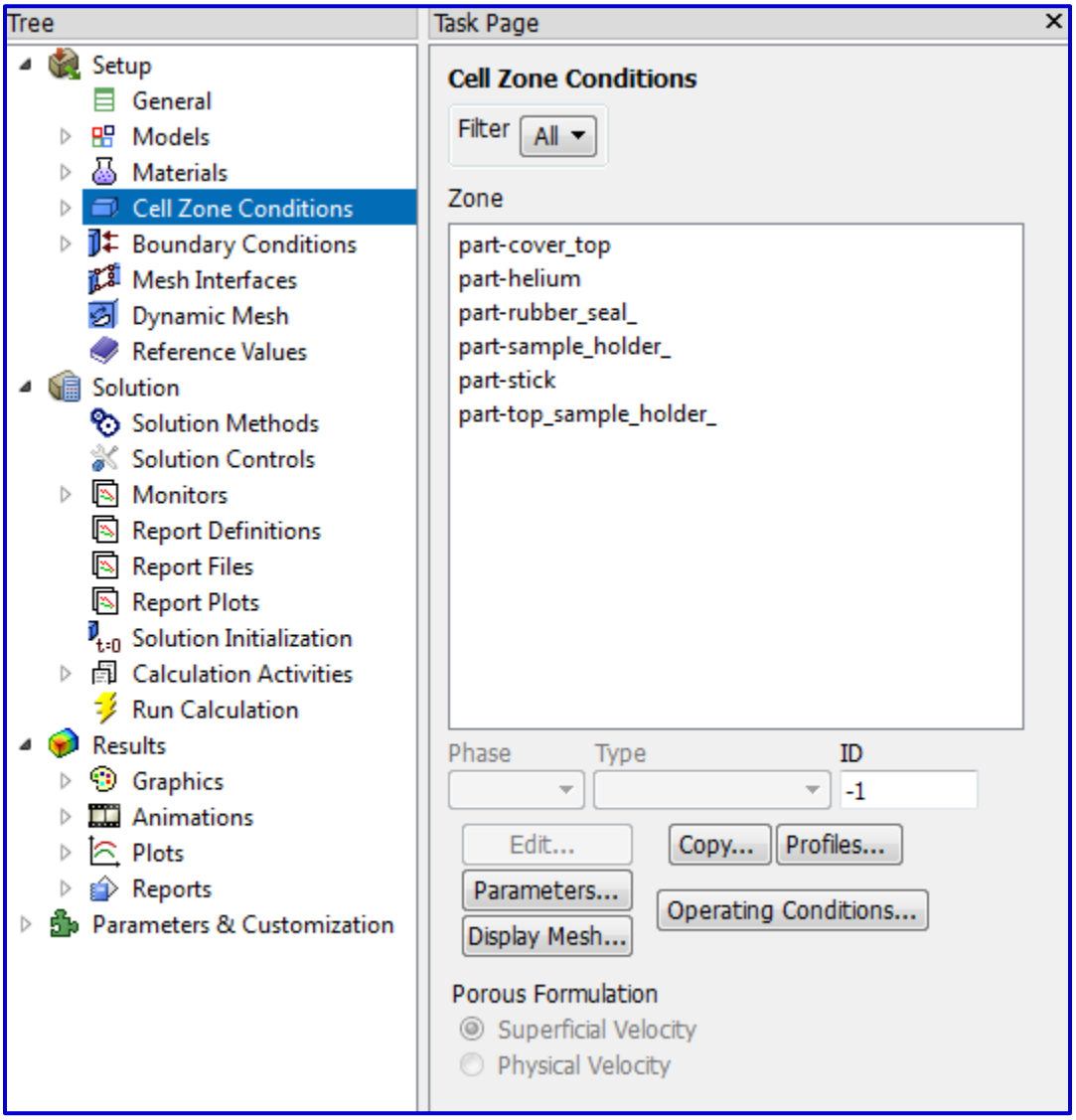

Figure 36. Cell zone condition screen [21]

Boundary Conditions

In this section each surface is assigned a boundary condition.

- Insulated if sample tube external
- Coupled if solid liquid interface
- Temperature of 300 K at top cover
- Temperature of 4.2 K at thermal strap

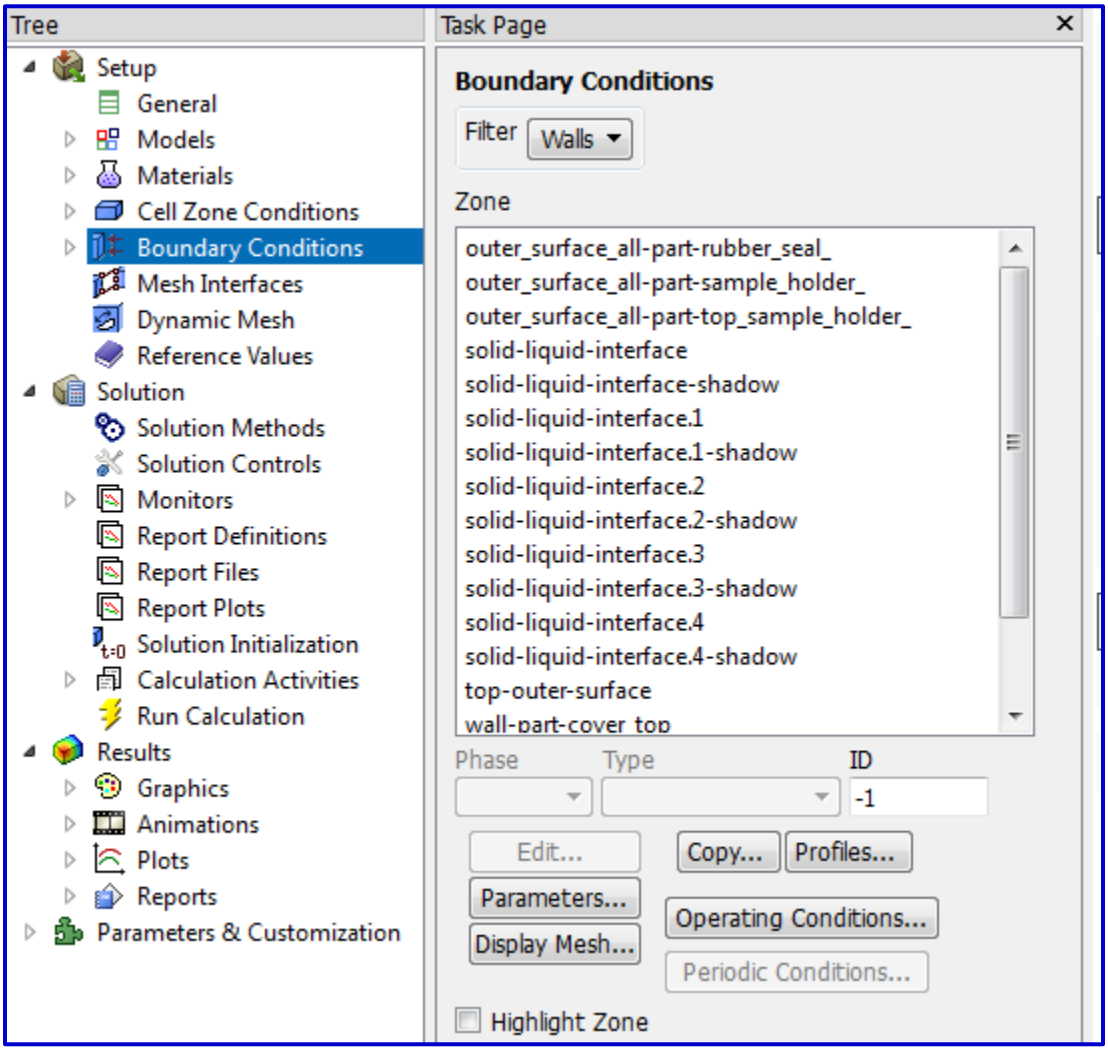

Figure 37. Boundary conditions screen [21]

Solution Method

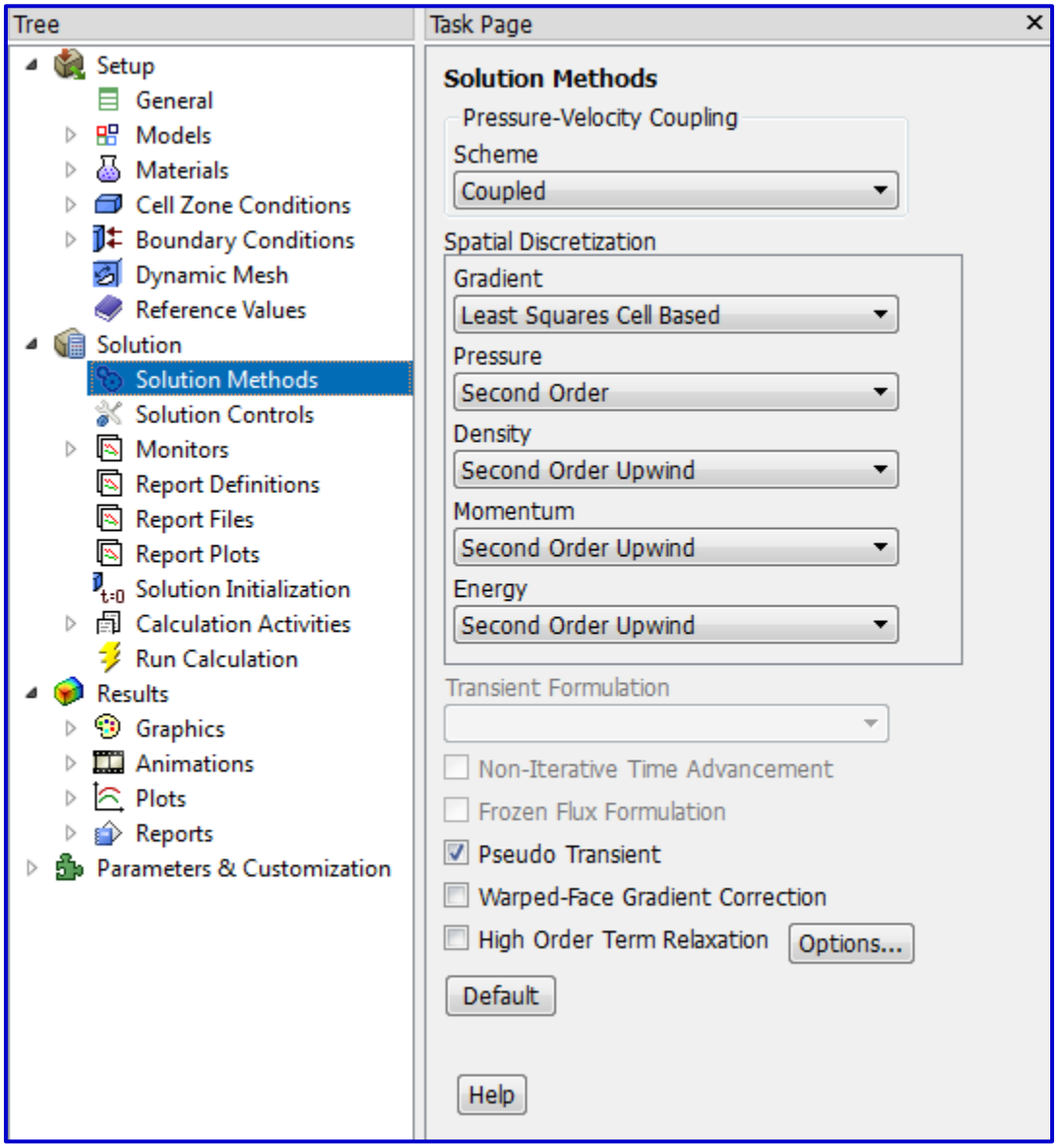

Figure 38. Solution method screen

Solution Control

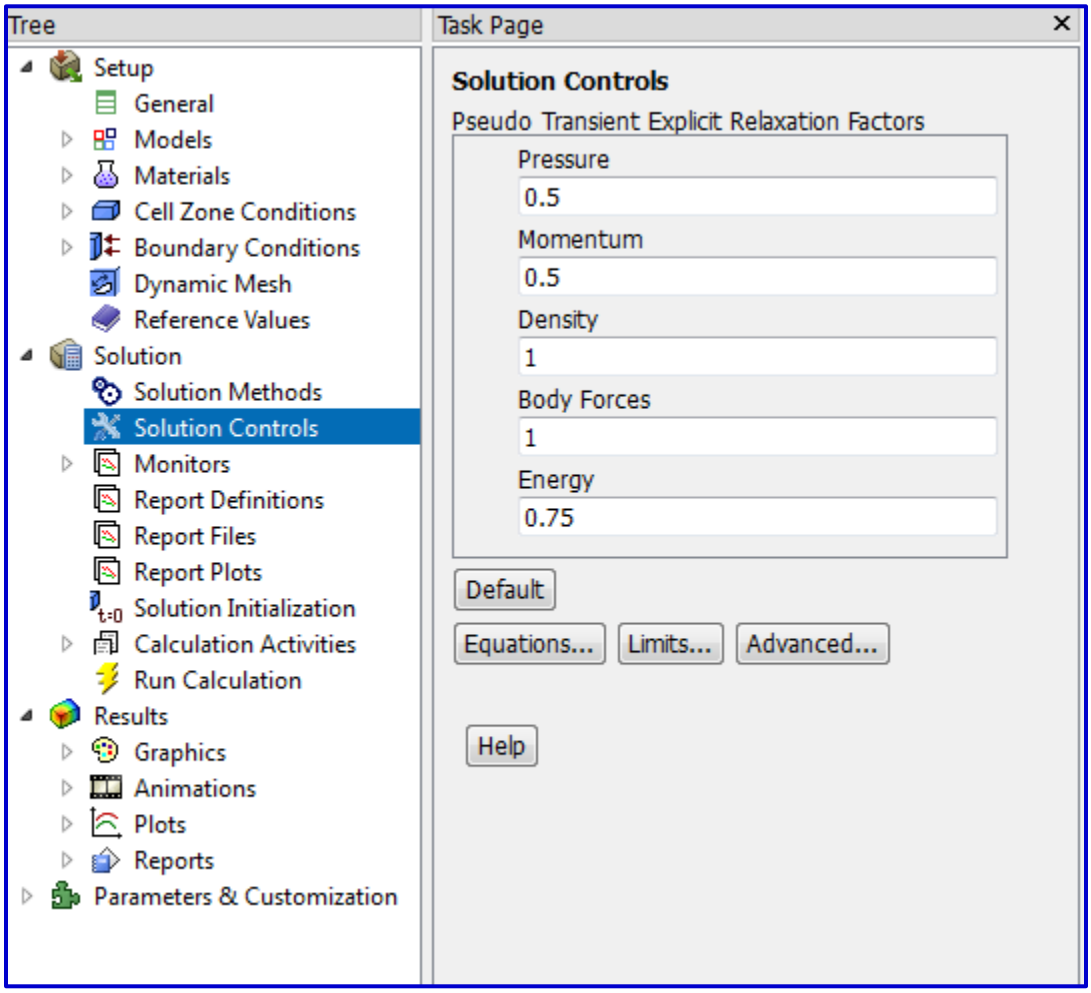

Figure 39. Solution control screen [21]

Solution Initialization

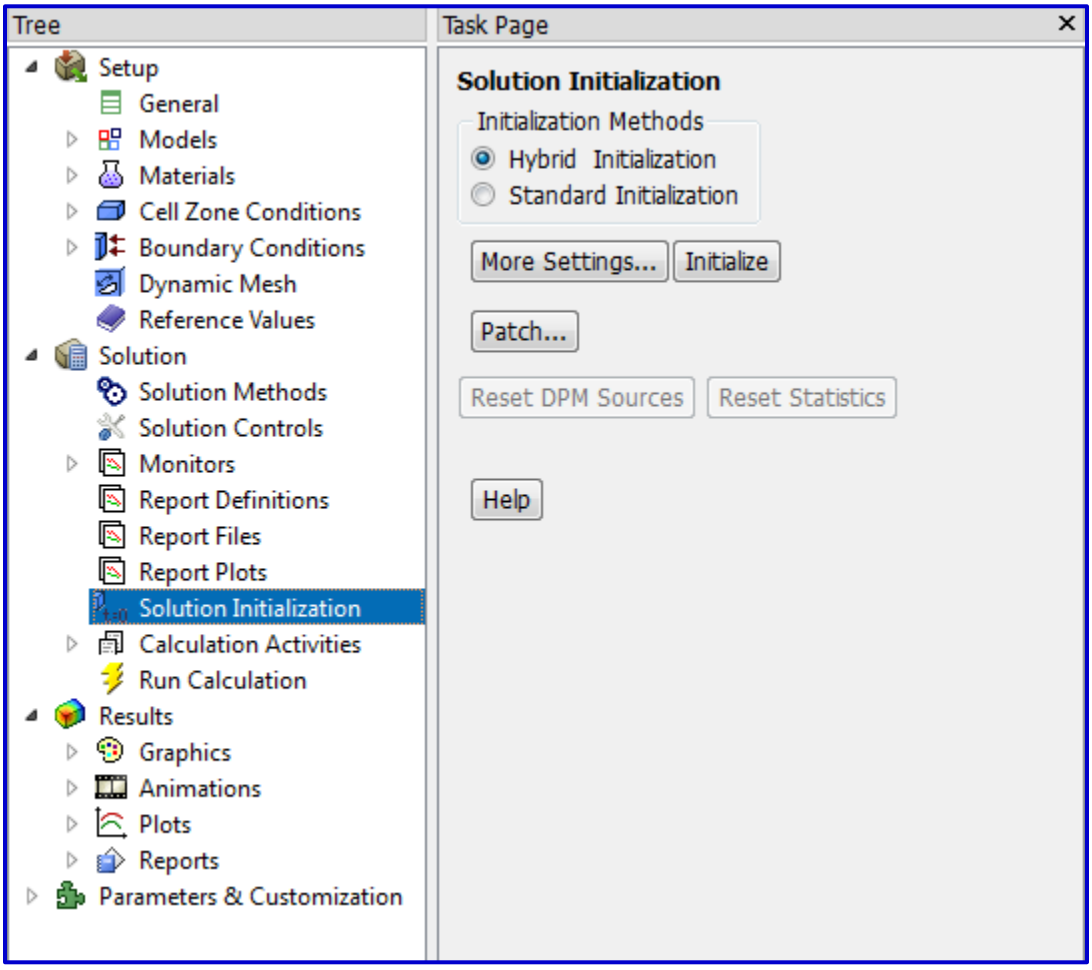

Figure 40. Solution initialization screen [21]

Run Calculation

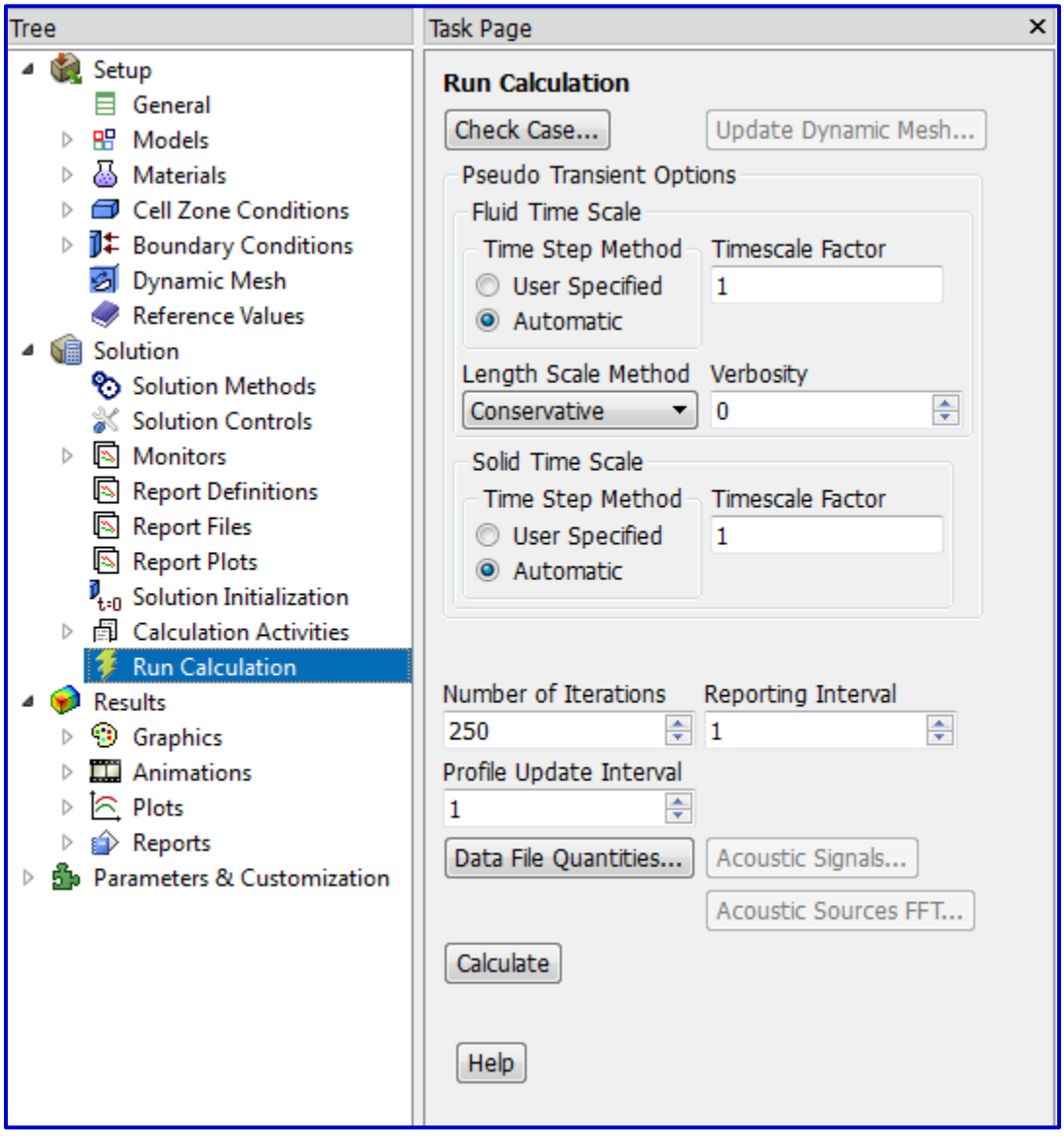

Figure 41. Run calculation screen [21]

Appendix 3.b: Fuent® UDF Script

A UDF script can be used to setup a power extraction at the thermal strap interface instead of applying a steady state temperature of 4.2 K. The power extraction of this UDF is shown in figure 9. The advantage of the UDF over directly applying the temperature boundary condition at the thermal strap is the fact that it captures the accuracy of the model physics. The temperature at the thermal strap was observed to increase when a heat load was introduced in the sample tube, therefore the temperature at the thermal strap interface is somewhat a function of the heat load and not completely independent of it as when a steady state temperature is applied.

UDF Script for Power Extraction

```
#include "udf.h"
#define c1 100.0

DEFINE_PROFILE(wall_flux, ft, var)
{

real temperature;
real imp_q;
real pos[ND_ND]; /* How 2D and 3D vectors are defined */

face_t f;

int ncount = 0;


begin_f_loop(f,ft) /* Special Fluent face loop macro */
{

temperature = F_T(f,ft);


/*y = -3.074E-12x6 + 2.996E-09x5 - 1.142E-06x4 + 2.169E-04x3 - 2.174E-02x2 + 1.168E+00x
- 2.720E+00*/
```

```
imp_q=-((-3.074E-12)*pow(temperature,6)+(2.996E-09)*pow(temperature,5)+(-1.142E-
06)*pow(temperature,4)+(2.169E-04)*pow(temperature,3)+(-2.174E-
02)*pow(temperature,2)+(1.168E+00)*temperature+(-2.720E+00))/0.002780021;

F_PROFILE(f,ft,var) = imp_q;

/*Message("qpp= %f\n",imp_q);*/


ncount += 1;

}

end_f_loop(f,ft)

Message("Number of cells %d, qpp= %f\n",ncount,imp_q);


}
```

ANSYS Results with UDF Boundary Condition Example

In this example the radiation effect is found to be negligible as the temperature increase due to radiation is in the order of 1 to 2 degrees. The UDF also allows capturing the amount of heat addition due to the radiation effect. It is found to be about 0.2 W

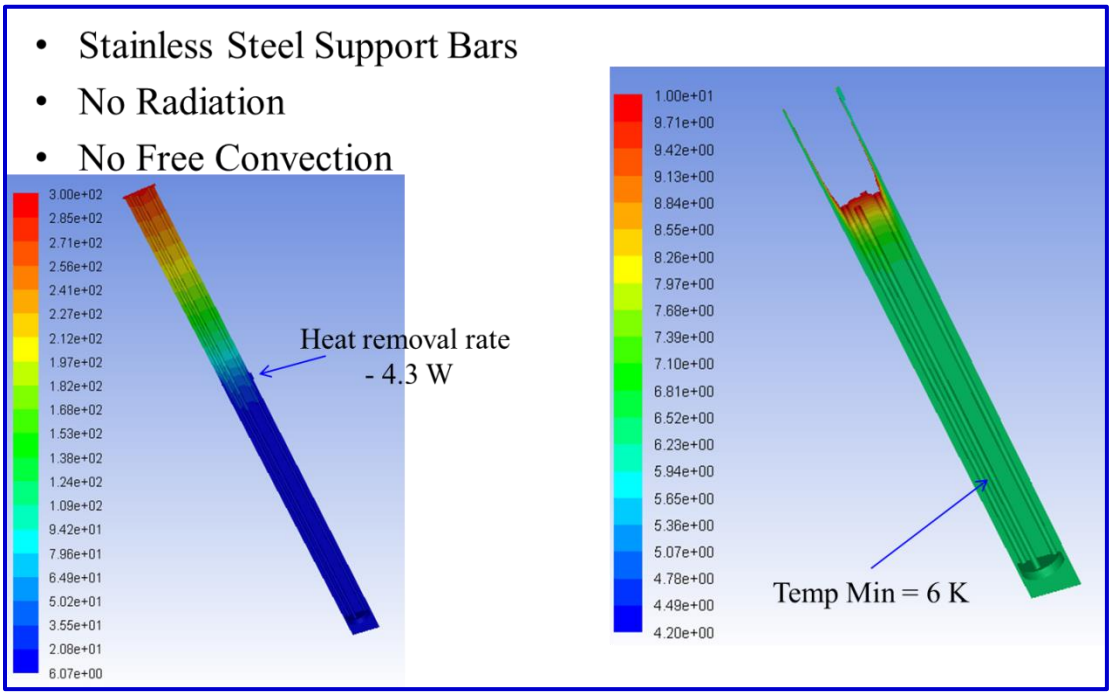

Figure 42. Stainless steel supported test rig with thermal strap power extraction

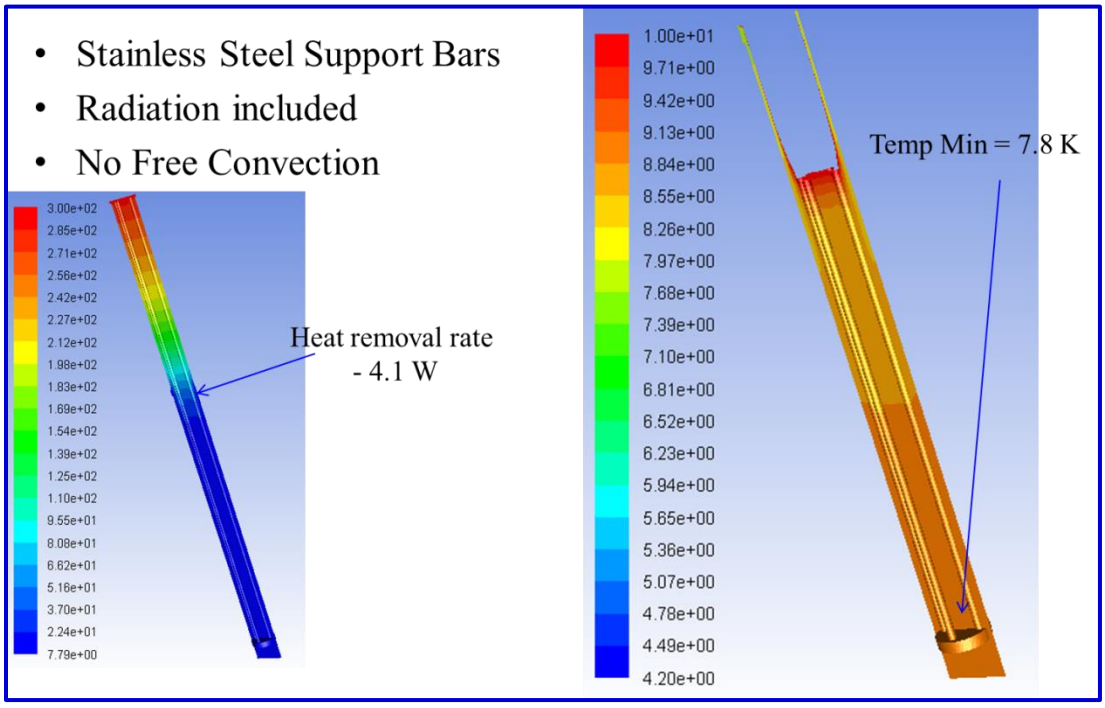

Figure 43. Stainless steel supported test rig with thermal strap power extraction

References

1. International Thermonuclear Experimental Reactor - https://en.wikipedia.org/wiki/ITER

2. Aeronautical Applications of High-Temperature Superconductors – Published by the NASA Lewis Center in Cleveland, Ohio – Aircraft Design, System and Operation Conference Seattle, Washington July 31- August 2, 1989.

3. The USS Gerald R. Ford (CVN-78) - Wikipedia, the free encyclopedia. https://en.wikipedia.org/wiki/USS_Gerald_R._Ford, accessed on 02/19/2016

4. . High Temperature Superconductivity - Wikipedia, the free encyclopedia https://en.wikipedia.org/wiki/High-temperature_superconductivity#Preparation_of_high-Tc_superconductors

5. Uses for Superconductors-Selected by Science Educators SC LINKS from NSTA- Last updated April 2015. http://www.superconductors.org/uses.htm, accessed on 02/19/2016

6. Wikipedia, the free encyclopedia. SCMaglev - https://en.wikipedia.org/wiki/SCMaglev , accessed on 02/19/2016

7. Janis Research Leading the design, development and production of cryogenic equipment since 1961. http://www.janis.com/Products/productsoverview/4KCryocooler/RDK-415DClosedCycleRefrigerator.aspx#

8. The Gifford-McMahon Refrigeration Cycles - http://www.arscryo.com/tech-notes/cryocooler-principle-of-operation.html

9. Edwards World Class Vacuum Solution - https://shop.edwardsvacuum.com/products/ts75d1002/view.aspx

10. F-70H and F-70L Helium Compressors, Operating Manual. Sumitotmo (SHI) Cryogenics of America, Inc. http://lmu.web.psi.ch/docu/manuals/bulk_manuals/OxfordInstruments/39370/F-70_Operating_Manual.pdf

11. Dimplex Thermal Solution - Koolant Kooler

12. Aeronautical Applications of HTS - http://ntrs.nasa.gov/archive/nasa/casi.ntrs.nasa.gov/19890016637.pdf

13. Cryogen Safety - https://www.ncnr.nist.gov/equipment/cryostats/CryogenSafety.pdf

14. Cryocooler, Wikipedia, the free encyclopedia.- https://en.wikipedia.org/wiki/Cryocooler

15. Cryocoolers - http://uspas.fnal.gov/materials/10MIT/Lecture_2.2.pdf

16. Fundamentals of Heat and Mass Transfer, Theodore L. Bergman, Adrienne S. Lavine, Frank P. Incropera / David P. Dewitt Seventh Edition John Wiley and Sons 2011

17. Heat Transfer Gregory Nellis, Sanford Klein, Cambridge University Press 2009

18. Experimental Techniques for Low - Temperature Measurement by Jack W. Ekin

19. Case Studies in Superconducting Magnets - Design and Operational Issues by Yukikazu Iwasa

20. Cryocooler Operating Principle - http://www.arscryo.com/tech-notes/cryocooler-principle-of-operation.htm

21. AC Loss and Stability of Superconducting Cables. https://www.utwente.nl/tnw/ems/Research/AC%20loss%20Twente%20Press/AC_loss_and_stability_of_superconducting_cables_for_fusion/

22. Ansys, Inc. Computer Software Company. http://www.ansys.com

23. Unigraphics NX: Siemens PLM Software, http://www.plm.automation.siemens.com/en_us/products/nx/index.shtml

24. SHI Cryogenics Group – Cryocooler Product Catalogue, Sumitomo Heavy Industries, ltd. http://www.shicryogenics.com//wp-content/uploads/2012/11/Cryocooler-Product-Catalogue.pdf

25. National Institute of Standards and Technology- Material Measurement Laboratory http://cryogenics.nist.gov/MPropsMAY/OFHC%20Copper/OFHC_Copper_rev.htm

27. The Gifford-McMahon Refrigeration Cycles: http://www.arscryo.com/tech-notes/cryocooler-principle-of-operation.html

28. Copper rod experiment in cryocooler – Performed by Federica Pierro.

29. Physics for Scientist and Engineers, Serway Jewett 6th edition, Thomson, Brooks Cole.

30. Simulation of Thermal Processes in Superconducting Pancake Coils Cooled by GM Cryocooler, M Lebiola, J Rymaszewiski and Korzeniewska, Institute of Electrical Engineering Systems, Lodz University of Technology, Stefanowskiego 18/22, 90-924 Lodz, Poland – Journal of Physics: Conference Series 494 (2014) 012018